國立臺灣大學基因體與系統生物學學位學程

碩士論文

Genome and Systems Biology Degree Program

National Taiwan University

Master Thesis

以數學模型解釋腫瘤壞死因子引起之細胞存活及細胞凋亡傳遞路徑之動態變化

Mathematical model to elucidate the dynamics of TNFα-induced apoptosis and pro-survival pathway

許哲瑜

Che-Yu Hsu

指導教授：許昭萍 博士

Advisor: Chao-Ping Hsu, Ph.D.

中華民國 105 年 6 月

June, 2016

doi:10.6342/NTU201602117

誌謝

能完成這篇論文，我要特別感謝我的指導教授許昭萍老師，也要感謝實驗室的每一位成員對我的支持與鼓勵，謝謝大家。

doi:10.6342/NTU201602117

中文摘要

腫瘤壞死因子(TNFα)於決定細胞凋亡(apoptosis)或存活的命運中扮演著重要角色。經由腫瘤壞死因子受體的激活，可導致 IIa 族複合蛋白(Complex IIa)的形成，並進一步引起第八及第三凋亡蛋白酶(Caspase-8 / Caspase-3)的活化與伴隨而來的細胞凋亡。此外活化的腫瘤壞死因子受體可以增加 I 族複合蛋白(Complex I)的形成，並能導致與核因子活化 B 細胞 κ 輕鏈增強子(NF-κB) 相關或不相關的細胞存活訊息傳遞路徑的活化。因為腫瘤壞死因子能同時啟動細胞存活或凋亡的傳遞路徑，所以細胞如何在此刺激下決定細胞走向存活或凋亡是一個困難的問題。

我們使用常微分方程模型來闡明經由腫瘤壞死因子刺激引起的複雜訊息傳遞路徑。我們的數學模型可以模擬在腫瘤壞死因子刺激下不同細胞個存活概率、第八及第三凋亡蛋白酶活性變化及第三凋亡蛋白酶活性達到最高變化之一半值所需之時間的分佈。這個模型提供我們研究在不同環境下細胞凋亡如何被驅使或阻斷的定量分析基礎。參數敏感性試驗顯示，在低濃度的腫瘤壞死因子刺激下，與 I 族複合蛋白引起 IκB kinase (IKK)活化及 IKK 引起之細胞質 B 淋巴细胞瘤-2 (Bcl-2c)活化相關之參數對於第三凋亡蛋白酶活化，扮演著重要的角色。我們引入治療指數來分析調整參數對於腫瘤壞死因子造成腫瘤細胞及正常組織細胞死亡的不同效應。這個模型能幫助我們更了解腫瘤壞死因子引起之細胞凋亡及細胞存活傳遞路徑，並且也可幫助我們挑選可應用於臨床治療之傳遞路徑目標。

關鍵字：腫瘤壞死因子、細胞凋亡、NF-κB 動態變化、模型

doi:10.6342/NTU201602117

Abstract

TNFα plays an important role in determining the cell fate of apoptosis or survival. Activation of TNFR1 by TNFα can result in complex IIa proteins formation, and trigger the Caspase-8 and Caspase-3 activation with subsequent apoptosis. On the other hand, active TNFR1 induced via TNFα can increase the formation of complex I , and complex I can result in both pro-survival signals mediated by NF-κB-dependent or NF-κB-independent signals transduction pathways. Since TNFα mediated paathways can activate both survival and apoptosis pathways, it is difficult to see how the decision for apoptosis or survive is made. We constructed an ordinary differential equations (ODEs) based mathematical model to elucidate the complex signal transduction pathway induced via TNFα stimulation. Our model can reproduce the experimental observation of cell viability probability, Caspase-3 /Caspase-8 activity, and delay time distribution. The model provides us a quantitative base to study how apoptosis is initiated or blocked under different conditions. Parametric sensitivity test reveals that these parameters involving the complex I mediated IKK activation and IKK mediated cytoplasm Bcl-2 regulation play more important roles in Caspase-3 activity under lower TNFα stimulation. Inhibiting these pathways could lead to increased apoptosis of cells under lower TNFα stimulation. A therapeutic index was developed to analyze the likelihood to kill more malignant cells than normal cells in modifying parameters in the model. The current model enables us to better understand TNFα-mediated apoptosis and pro-survival pathway quantitatively and help to identify targets for therapeutic application.

Key words: TNFα, apoptosis, NF-κB dynamics, mathematical model

doi:10.6342/NTU201602117

CONTENTS

doi:10.6342/NTU201602117

doi:10.6342/NTU201602117

LIST OF FIGURES

doi:10.6342/NTU201602117

doi:10.6342/NTU201602117

LIST OF TABLES

doi:10.6342/NTU201602117

Chapter 1 Introduction

Programmed cell death is an important and common process in various multicellular organisms, and apoptosis is one form of programmed cell death involving interactions among different substrates, caspases, and cysteine proteases [1]. The most characterized features of apoptosis are chromatin condensation, nuclear fragmentation, membrane blebbing, cell shrinkage, and formation of apoptotic bodies [2]. Abnormal regulation of apoptosis is associated with serious diseases as diverse as cancer and autoimmunity.

There are two main apoptotic pathways, the extrinsic pathway which involves death receptors, and the intrinsic pathway which involves mitochondria [3]. In the extrinsic apoptosis pathway, binding of ligands (TNFα, TRAIL, CD95L/ FasL) to cell membrane receptors (TNFR1, TNFR2, TRAIL receptor 1, TRAIL receptor 2) will trigger the formation of the death-inducing signaling complex (DISC) and subsequent caspase activation. The intrinsic pathway is initiated by reactive oxygen species (ROS) formation, chemotherapeutic drugs, irradiation, and growth factor withdrawal. The stimuli in intrinsic pathways results in mitochondrial outer membrane permeabilization (MOMP), subsequent cytochrome-c release and caspase activation[4]. One of the most famous extrinsic apoptosis pathways is tumor necrosis factor-α (TNFα)

doi:10.6342/NTU201602117

triggered apoptosis pathway.

1.1 Overview of TNFα mediated apoptosis

Pathways of TNFα mediated apoptosis included in the present work are included in Fig.1 The initial step of TNFα triggered apoptosis is the binding of TNFα to TNFα receptor 1 (TNFR1) and leads to the trimerization of TNFR1 which further combine with TNF receptor 1-associated protein (TRADD), TNF Receptor-associated factor 2 (TRAF2) and receptor-interacting protein 1 (RIP1) and cellular inhibitor of apoptosis 1 and 2 (cIAP1 and cIAP2) to form the complex I. Complex I is then internalized to cytoplasm from the cell membrane[5-7], and by further recruiting FADD proteins and procaspase-8/procaspase-10, complex IIa is formed. Procaspase-8 in complex IIa undergoes caspase processing and generate active Caspase-8, which plays an important role in the execution of extrinsic apoptosis. One way to trigger apoptosis via Caspase-8 is to directly activate Caspase-3. Another way is to mediate the cleavage of the pro-apoptotic Bcl-2 family member proteins (Bid) into truncated Bid proteins (tBID). tBID is then translocated into the mitochondria and activate the pro-apoptotic Bcl-2 family members, Bax proteins (Fig. 1]. The active form of Bax facilitates mitochondrial outer membrane permeabilization (MOMP), enabling the release of proteins such as Cytochrome c from the mitochondrial intermembrane space into cytoplasm [8].

doi:10.6342/NTU201602117

Released cytochrome c form active apoptosome and the second mitochondria-derived activator of caspase proteins (Smac), both facilitate the activation of Caspase-3. The active form of Caspase-3 will lead to rapid cleavage of Caspase-3 substrates and cell death (Fig. 1) [8].

In addition to apoptosis pathway, complex I also induces phosphorylation of IκB kinase complex (IKK) and subsequent activation of both NF-κB-dependent and NF-κB-independent pro-survival pathways [6, 7], as discussed below.

1.2 Overview of TNFα mediated pro-survival pathway

1.2.1 NF-κB-dependent pro-survival pathway

TNFα receptor 1 (TNFR1) is trimeric in its active form. After being triggered by the binding of TNFα, TRADD, TRAF2 and RIP1 proteins are recruited to TNFR1 and form complex I. The Lys63 poly-ubiquitin chain on the Lys377 of RIP1 protein in complex I will then be initiated within minutes [9]. The Lys63 polyubiquitin chain serves as a platform for binding of NEMO in the IκB kinase (IKK) complex. This platform recruits IKK complex and allows it to be activated by phosphorylation. The active IKK subsequently phosphorylates the IκBa proteins, the inhibitor of NF-κB. The

doi:10.6342/NTU201602117

phosphorylated IκBa undergoes degradation, frees the NF-κB in cytoplasm and allows NF-κB migration to the nucleus. NF-κB binds to target promotors and facilitates the transcription many target genes. Among them, c-IAP1, c-IAP2, XIAP, and c-FLIP, are found to be anti-apoptotic as then can block the activation of Caspase-3 (Fig. 2).

1.2.2 NF-κB -independent prosurvival pathway

The TNFα can also mediate the pro-survival signals without the assistance of NF-κB. According to the work of Yan et al. [6], the active IKK proteins triggered via TNFα stimulation inactivates the BH3-only protein and subsequently suppressed the TNFα–induced extrinsic apoptosis (Fig. 3). The active form of IKK proteins phosphorylates the BAD protein, and down-regulates the BAD mediated inhibition of the pro-survival signal of Bcl-XL proteins. The free-form of Bcl-XL can block the formation of tBID and inhibit the subsequent MOMP and apoptosis. The phosphorylation site of BAD is at serine-26 (Ser26) and primes it for inactivation of binding with Bcl-XL proteins.

Recent works using dynamic model depicted how TNFα–mediated NF-κB pathway works and how extrinsic apoptosis pathway executes following caspase activation steps [5, 10, 11]. Although many studies comprehensively described TNFα mediated

doi:10.6342/NTU201602117

apoptosis and pro-survival pathways independently [9, 12-15], quantitative understanding of how TNFα mediates apoptosis and pro-survival pathways simultaneously has not been established clearly. It has been unclear on the decision for apoptosis or survival. How is apoptosis initiated or blocked under in different conditions? What are the rate-limiting steps in the processes?

Due to the complex nature of TNFα mediated apoptosis and pro-survival pathways, the emerging tools of systems biology can be useful to study the system quantitatively and provide us new insights of this fascinating system. In the present study using current literature we construct a mathematical model to elucidate the dynamic behavior of TNFα mediated apoptosis and pro-survival pathways. With this mathematical model, we hope to explore the possibilities and boundaries for the cell fates.

doi:10.6342/NTU201602117

Chapter 2 Mathematical model of apoptosis

Mathematical tools are useful to study the dynamics of the biological systems comprising the of various biochemical reactions. Ordinary differential equations (ODEs) are most commonly used approach to study the dynamical behavior of the biochemical reactions in the system. An ODE normally expresses the time derivative of a dynamic variable in terms of a function, usually nonlinear, of this variable. For example, if [E], [S], and [C] are concentrations of enzyme, substrate, and complex, respectively,

$$\mathrm{E} + \mathrm{S} \underset{k_2}{\overset{k_1}{\rightleftarrows}} \mathrm{C} \xrightarrow{k_3} \mathrm{P}$$

then the dynamical system describes Michaelis-Menten kinetics [16].

$$\frac{\mathrm{d[E]}}{\mathrm{dt}} = -k_1[\mathrm{E}][\mathrm{S}] + k_2[\mathrm{C}] \tag{1}$$

$$\frac{\mathrm{d[S]}}{\mathrm{dt}} = -k_1[\mathrm{E}][\mathrm{S}] + k_2[\mathrm{C}] \tag{2}$$

$$\frac{\mathrm{d[C]}}{\mathrm{dt}} = k_1[\mathrm{E}][\mathrm{S}] - k_2[\mathrm{C}] - k_3[\mathrm{C}] \tag{3}$$

$$\frac{d[\mathrm{P}]}{dt} = k_3[\mathrm{C}] \tag{4}$$

In this system, rates k_1 and k_2 (k_3) are reaction rates, which are regarded as model parameters. ODE has been a powerful tool in analyzing dynamics, since (i) vast mathematical apparatus (bifurcation diagrams and phase portraits, perturbation theory, and numerical analysis) have been developed to solve them; (ii) solving ODEs is fast

doi:10.6342/NTU201602117

and easy with much available user-friendly software; and (iii) their solutions provide very detailed mechanistic insight. However, additional assumptions and problems exist for using ODEs to describe systems in a cell. Chemicals are assumed to be well mixed in the cell. Their spatial gradients are neglected. Moreover, detailed information about molecular interactions are needed for the proper reaction kinetics in the ODEs. It often requires many data to validate the model [16]. In many cases quantitative measurement helps confining the reaction rates and other parameters. Qualitative mutant phenotypes have also been useful in building models and finding parameters.

TNFα mediated pro-survival and apoptosis pathways comprises a network of interacting signal mediators, which contains positive or negative feedback loops and crossing over of distinct pathways. We constructed a complete mathematical model to describe TNFα mediated pro-survival and apoptosis networks based on the established TNFα-induced NF-κB signaling transduction model developed by Tay et al. [9] and extrinsic apoptosis reaction model by Allbeck et al. [17]. Below are the detailed ODEs for the concentration of each component in the model, followed by the discussion of detailed model settings.

doi:10.6342/NTU201602117

2.1 Model for TNFα-induced NF-κB signaling transduction Pathway

Tay et al. developed a mathematical model for TNFα-induced NF-κB signal transduction pathway [5] . In this pathway, the formation of active TNFα receptor complex requires trimerization of TNFR1 and the binding of the TNFα to TNFR1. The active TNFα receptor recruits the adapter protein TRADD, which further serves as an assembly platform for TRAF2 and RIP1. The recruited proteins at the intra-cellular domain of TNFR1 will become the complex I. The neutral form of IKKK (IKK kinase) molecules, IKKKn, migrates toward the complex I and transforms to an active form of IKKK (IKKKa). IKKKa molecules further activate neutral form of IKK molecules (IKKn) to an active form of IKK (IKKa). As the activation of IKK requires phosphorylation at both Ser177 and Ser181 sites, they assume that IKK activation rate is proportional to square of IKKKa. Furthermore, IKKa phosphorylates IκBα molecules, which leads to ubiquitination and degradation of IκBα molecules. In resting cells, the unphosphorylated IκBα binds to NF-κB and remains inactive in the cytoplasm. IKKa mediated phosphorylation of IκBα leads to its degradation and releases the main activator NF-κB.

The free NF-κB enters the nucleus and triggers transcription of the two inhibitors (IκBα and A20) and other pro-survival genes. The first inhibitor is IκBα, which will

doi:10.6342/NTU201602117

help export of NF-κB out of the nucleus and subsequently bind to NF-κB in cytoplasm. The second inhibitor protein, A20 lowers the complex I mediated IKKK-IKK activation by initiating degradation of one key complex I protein, RIP1, and associating with IKK further enhance IKKa conversion to catalytically inactive form IKK (IKKi). Other NF-κB target genes include anti-apoptotic members of the IAP family (c-IAP1, c-IAP2, XIAP and Survivin) and FLIP, which inhibit various pro-apoptotic proteins. In addition to pro-survival genes, according to Pekalski et al [10], NF-κB also serves as a primary transcription factor for TNFα, leading to TNFα autocrine and paracrine signaling. The equations describing the TNFα-induced NF-κB signaling transduction pathway are included in Eqs 5 to 31 in our model. We note that in the present work, the amount of each component is in the units of copies per cell.

$$\frac{d(\mathrm{TNFRa})}{dt} = \mathrm{TNF} \times \mathrm{csec} \times \frac{\mathrm{TNFRi}}{(\mathrm{TNFRi+cb})} + \mathrm{kb} \times \mathrm{TNF\_ext} \times \mathrm{TNFRi} - \mathrm{kf} \times \mathrm{TNFRa} \quad (5)$$

$$\frac{d(\mathrm{IKKKa})}{dt} = \mathrm{ka} \times \mathrm{TNFRa} \times \mathrm{IKKKn} \times \frac{\mathrm{ka20}}{(\mathrm{ka20+A20})} - \mathrm{ki} \times \mathrm{IKKKa} \quad (6)$$

$$\frac{d(\mathrm{IKKa})}{dt} = \mathrm{IKKKa}^2 \times \mathrm{k1} \times \mathrm{IKKn} - \mathrm{k3} \times \mathrm{IKKa} \times \frac{(\mathrm{k2+A20})}{\mathrm{k2}} \quad (7)$$

$$\frac{d(\mathrm{IKKn})}{dt} = \mathrm{k4} \times \mathrm{IKKii} - \mathrm{k1} \times \mathrm{IKKKa}^2 \times \mathrm{IKKn} \quad (8)$$

$$\frac{d(\mathrm{IKKi})}{dt} = \mathrm{k3} \times \mathrm{IKKa} \times \frac{(\mathrm{k2+A20})}{\mathrm{k2}} - \mathrm{k4} \times \mathrm{IKKi} \quad (9)$$

$$\frac{d(\mathrm{A20\_mRNA})}{dt} = \mathrm{c1} \times \mathrm{G\_A20} - \mathrm{c3} \times \mathrm{A20\_mRNA} \quad (10)$$

$$\frac{d(\mathrm{A20})}{dt} = \mathrm{c4} \times \mathrm{A20\_mRNA} - \mathrm{c5} \times \mathrm{A20} \quad (11)$$

doi:10.6342/NTU201602117

$$\frac{d(\mathrm{I}\kappa B\alpha\_\mathrm{mRNA})}{dt} = \mathrm{c1}\times \mathrm{G\_I}\kappa B\alpha - \ \mathrm{c3}\times \mathrm{I}\kappa B\alpha\_\mathrm{mRNA} \quad (12)$$

$$\frac{d(\mathrm{I}\kappa B\alpha)}{dt} = \mathrm{c4}\times \mathrm{I}\kappa B\alpha\_\mathrm{mRNA} - \mathrm{a2}\times \mathrm{IKKa}\times I\kappa B\alpha - \mathrm{a1}\times I\kappa B\alpha \times \mathrm{NF}\kappa B - \mathrm{c5a}\times I\kappa B\alpha$$
$$-\mathrm{i1a}\times \mathrm{I}\kappa \mathrm{B}\alpha + \mathrm{e1a}\times I\kappa B\alpha n \quad (13)$$

$$\frac{d(\mathrm{I}\kappa B\alpha \mathrm{n})}{dt} = \mathrm{i1a}\times \mathrm{I}\kappa B\alpha - \mathrm{a1}\times \mathrm{kv}\times \mathrm{I}\kappa B\alpha \mathrm{n}\times \mathrm{NF}\kappa \mathrm{Bn} - \mathrm{e1a}^{*}\mathrm{I}\kappa B\mathrm{an} \quad (14)$$

$$\frac{d(\mathrm{I}\kappa B\alpha p)}{dt} = \mathrm{a2}\times \mathrm{IKKa}\times \mathrm{I}\kappa B\alpha - \mathrm{tp}\times \mathrm{I}\kappa B\alpha p \quad (15)$$

$$\frac{d(\mathrm{NF}\kappa B)}{dt} = \ \mathrm{c6a}\times (NF\kappa B : I\kappa B\alpha) - \mathrm{a1}\times \mathrm{I}\kappa B\alpha \times NF\kappa B + \mathrm{tp}\times (NF\kappa B : I\kappa B\alpha p)$$
$$-\mathrm{i1}\times \mathrm{NF}\kappa \mathrm{B} \quad (16)$$

$$\frac{d(\mathrm{NF}\kappa Bn)}{dt} = \ \mathrm{i1}\times NF\kappa B - \text{-}\mathrm{a1}\times \mathrm{kv}\times \mathrm{I}\kappa B\alpha n\times NF\kappa Bn \quad (17)$$

$$\frac{d((NF\kappa B : I\kappa B\alpha))}{dt} = \mathrm{a1}\times \mathrm{I}\kappa B\alpha \times NF\kappa B - \mathrm{c6a}\times (NF\kappa B : I\kappa B\alpha)$$
$$-\mathrm{a3}\times \mathrm{IKKa}\times (NF\kappa B : I\kappa B\alpha) + \mathrm{e2a}\times (NF\kappa B : I\kappa B\alpha n) \quad (18)$$

$$\frac{d((NF\kappa B : I\kappa B\alpha p))}{dt} = \mathrm{a3}\times \mathrm{IKKa}\times (NF\kappa B : I\kappa B\alpha) - \mathrm{tp}\times (NF\kappa B : I\kappa B\alpha p) \quad (19)$$

$$\frac{d(\mathrm{TNF\_mRNA})}{dt} = \ \mathrm{lambda}\times \mathrm{G\_TNFa}\times \mathrm{IKKa} - \mathrm{c3t}\times \mathrm{TNF\_mRNA} \quad (20)$$

$$\frac{d(\mathrm{TNF})}{dt} = \ \mathrm{c4t}\times \mathrm{TNF\_mRNA} - \mathrm{c5t}\times \mathrm{TNF} - \mathrm{csec}\times \mathrm{TNF} \quad (21)$$

$$\frac{d(\mathrm{TNF\_ext})}{dt} = \ -\mathrm{cdeg}\times \mathrm{TNF\_ext} \quad (22)$$

$$\frac{d(\mathrm{G\_A20})}{dt} = \mathrm{q1}\times \mathrm{NFkBn}\times (\mathrm{NA} - \mathrm{G\_A20}) - \mathrm{q2}\times IkBan\times \mathrm{G\_A20} \quad (23)$$

$$\frac{d(\mathrm{G\_I}\kappa \mathrm{B}\alpha)}{dt} = \mathrm{q1}\times \mathrm{NF}\kappa \mathrm{Bn}\times (\mathrm{NI} - \mathrm{G\_I}\kappa \mathrm{B}\alpha) - \mathrm{q2}\times I\kappa B\alpha n\times \mathrm{G\_I}\kappa \mathrm{B}\alpha \quad (24)$$

$$\frac{d(\mathrm{G\_TNF}\alpha)}{dt} = \mathrm{q1t}\times \mathrm{NF}\kappa \mathrm{Bn}\times (\mathrm{NT\text{-}G\_TNF}\alpha) - (\mathrm{q2tt}+\mathrm{q2}\times I\kappa B\alpha n)\times \mathrm{G\_TNF}\alpha \quad (25)$$

$$\frac{d(\mathrm{TNFRi})}{dt} = \ \mathrm{kf}\times \mathrm{TNFRa} - \mathrm{TNF}\times \mathrm{csec}\times \frac{\mathrm{TNFRi}}{(\mathrm{TNFRi}+\mathrm{cb})} - \mathrm{kb}\times \mathrm{TNF\_ext}\times \mathrm{TNFRi} \quad (26)$$

doi:10.6342/NTU201602117

$$\frac{d(\mathrm{IKKKn})}{dt} = \mathrm{ki}\times\mathrm{IKKKa} - \mathrm{ka}\times\mathrm{TNFRa}\times\mathrm{IKKKn}\times\frac{\mathrm{ka20}}{(\mathrm{A20+ka20})} \quad (27)$$

$$\frac{d(\mathrm{IKKii})}{dt} = \mathrm{k4}\times\mathrm{IKKi} - \mathrm{k4}\times\mathrm{IKKii} \quad (28)$$

$$\frac{d((\mathrm{NF}\kappa\mathrm{Bn:IkB}\alpha\mathrm{n}))}{dt} = \mathrm{a1}\times\mathrm{kv}\times\mathrm{I}\kappa\mathrm{B}\alpha\mathrm{n}\times\mathrm{NF}\kappa\mathrm{Bn} - \mathrm{e2a}\times(\mathrm{NF}\kappa\mathrm{Bn:I}\kappa\mathrm{B}\alpha\mathrm{n}) \quad (29)$$

$$\frac{d(\mathrm{G\_Xiap})}{dt} = \mathrm{q1iap}\times\mathrm{NF}\kappa\mathrm{Bn}\times(\mathrm{NI\text{-}G\_Xiap}) - \mathrm{q2iap}\times I\kappa Ban\times\mathrm{G\_Xiap} \quad (30)$$

$$\frac{d(\mathrm{XIAP\_mRNA})}{dt} = \mathrm{c1iap}\times\mathrm{G\_Xiap} - \mathrm{c3iap}\times\mathrm{XIAP\_mRNA} \quad (31)$$

In the model developed by Tay et al. [9], the authors introduced extrinsic noise to account the different levels of TNFR1 observed across the population. They assumed that the total amount of TNFR1 in each cell follows the log normal distribution, defined as:

$$f = \frac{1}{x\sigma\sqrt{2\pi}}\mathrm{Exp}\left(-\frac{(\ln(x)-\mu)^2}{2\sigma^2}\right) \quad (32)$$

where parameters used are,

$$\sigma = \sqrt{2},\ \mu = -1$$

With x obtained following the distribution as in Eq 32, the amount of TNFR1 is Ax, where A is determined based on previous understanding of TNFR1 expression in various work. In this study, it is 3000, 1000, and 150 for MEF, HT1080, and HeLa cells. With this distribution, the mean value of x is 1, which corresponds to TNFR1 number is A, the median value for TNFR1 is $A\times e^{-1}$, and the corresponding variance is

doi:10.6342/NTU201602117

$A^2 \times (e^2 - 1)$.

Using high-throughput microfluidic cell culture, fluorescence microscopy, and quantitative gene expression analysis, Tay et al. validated their mathematical model and investigate how single cells of NIH/3T3 cell line respond to different concentrations of TNFα. The found that the response in NF-κB activation is heterogeneous among cells, and the fractions of active cells were 0, 0.1, 0.9, and 1 under the stimulation 0.01, 0.1, 1, 10 ng/ml TNFα, respectively. The observation that fewer active cells respond at lower doses of TNFα is the major result in NF-κB response to TNFα stimulation in single-cell level, which we aim to reproduce in the current model. [9].

2.2 Extrinsic apoptosis reaction model

One model describing TRAIL ligand triggered extrinsic apoptosis followed the one developed by Albeck et al. [17] In this model, the signal of extrinsic apoptosis pathway is initiated via TRAIL ligand binding to TRAIL receptors and the subsequent recruitment of proteins to intracellular domain of TRAIL receptors further activates the formation of DISC (Death-Inducing Signaling Complex). The DISC allows the procaspases-8 and procaspases-10 to undergo dimerization and autocatalyzation, and give rise to formation of Caspases-8/10, which can be blocked by FLIP. Caspases-8 and

doi:10.6342/NTU201602117

-10 could directly cleave and activate effector Caspases-3/7, leading to cell apoptosis. Caspases-3/7 mediated apoptosis could be inhibited by XIAP. Besides, Caspases-8 /-10 could cleave Bid into truncated Bid (tBID), which translocates to the mitochondria and activate pro-apoptotic Bcl-2 family members Bax and Bak (Bax*). The antiapoptotic Bcl-2 family proteins in the cytosol can form dimers with tBID and decrease the amount of tBID translocating into mitochondria. Bax* proteins will further form dimers (Bax2*) or tetramers (Bax4*). The Bax*, Bax2*, and Bax4* will create pores in the mitochondrial membrane and further cause MOMP with the release of Smac and cytochrome c into the cytosol. The antiapoptotic Bcl-2 family proteins in the mitochondrial part could inhibit the pores formation by Bax*, Bax2*, and Bax4*. Cytochrome c promotes assembly of Caspase-9 (C9)-containing apoptosome, and Smac displaces XIAP from its inhibitory effect on Caspase-3. Activation of Caspase-3 leads to rapid cleavage of Caspase-3 substrates and cell death.

In building the model, Albeck et al. [17] uses data derived from live-cell imaging, flow cytometry, and immunoblotting of cells perturbed by protein depletion and overexpression to train the parameters. They first developed the live-cell reporters specific to initiator and effector caspases, including three fluorescent fusion proteins. The effector caspase reporter protein (EC-RP) is composed of a Forster Resonance Energy Transfer (FRET) donor-acceptor pair (CFP and YFP) which was connected via a

doi:10.6342/NTU201602117

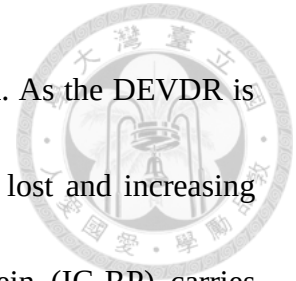

flexible linker that contains the caspase cleavage sequence DEVDR. As the DEVDR is cleaved proportion to the activity of Caspase-3, energy transfer is lost and increasing CFP signal can be observed. The initiator caspase reporter protein (IC-RP) carries copies of sequence, IETD, in the linker of FRET donor-acceptor pair. The IETD is efficiently cleaved by Caspase-8, but poorly by Caspases-3. The third reporter was constructed for MOMP localizes to the inter-membrane space. They treated the reporters incorporated HeLa cells with TRAIL and cycloheximide, and recorded the fluorescence signals every 3 min over an 8-12 hrs.

The model developed Albeck et al. [17] had three simplifications to reduce the number of species and free parameters. The first is to simplify the detail of DISC and apoptosome assembly. The second is to omit the effect of cycloheximide effects except the apoptosis sensitizing. The third was proteins with similar biochemical activities were represented by single species: C8 and caspase-10 (C10) by C8 alone; C3 and C7 by C3 alone; and Bcl-2-like family of proteins by three prototypical examples: Bid, a pro-apoptotic ‘‘activator,’’ Bcl-2, an apoptosis inhibitor, and Bax, a pore-forming protein. Here we follow Albeck’s settings and assumptions in the present work. The TNFα-induced extrinsic signaling transduction pathway we employed in this work are as listed in Eqs 33 to 83.

doi:10.6342/NTU201602117

$$\frac{d(\mathrm{R^*})}{dt} = \mathrm{kc(1)\times c4rac\times TNFRa - k(2)\times R^*\times flip+k\_(2)\times(flip:R^*) - k(3)\times R^*\times pC8+k\_(3)\times(R^*:pC8)+kc(3)\times(R^*:pC8) - c5rac\times R^*} \quad (33)$$

$$\frac{d(\mathrm{flip})}{dt} = \mathrm{c4iflip}\times\frac{\mathrm{XIAP\_mRNA}}{\mathrm{Kflip+XIAP\_mRNA}} - \mathrm{k(2)\times R^*\times flip + k\_(2)\times(flip:R^*)} \quad (34)$$

$$\frac{d((\mathrm{flip:R^*}))}{dt} = \mathrm{k(2)\times R^*\times flip - k\_(2)\times(flip:R^*)} \quad (35)$$

$$\frac{d(\mathrm{pC8})}{dt} = \mathrm{k\_(3)\times(R^*:pC8) - k(3)\times R^*\times pC8} \quad (36)$$

$$\frac{d((\mathrm{R^*:pC8}))}{dt} = \mathrm{k(3)\times R^*\times pC - k\_(3)\times(R^*:pC8) - kc(3)\times(R^*:pC8)} \quad (37)$$

$$\frac{d(\mathrm{C8})}{dt} = \mathrm{kc(3)\times(R^*:pC8) - k(4)\times C8\times Bar+ k\_(4)\times(Bar:C8) - k(5)\times C8\times pC3 +k\_(5)\times(C8:pC3)+kc(5)\times(C8:pC3) - k(10)\times C8\times Bid +k\_(10)\times C8:Bid+ kc(10)\times(C8:Bid) - kcDEG37(3)\times C8} \quad (38)$$

$$\frac{d(\mathrm{Bar})}{dt} = \mathrm{k\_(4)\times(Bar:C8) - k(4)\times C8\times Bar} \quad (39)$$

$$\frac{d((\mathrm{Bar:C8}))}{dt} = \mathrm{k(4)\times C8\times Bar - k\_(4)\times(Bar:C8)} \quad (40)$$

$$\frac{d(\mathrm{pC3})}{dt} = \mathrm{k\_(5)\times(C8:pC3) - k(25)\times pC3\times Apop+k\_(25)\times(Apop:pC3) - k(5)\times C8\times pC3} \quad (41)$$

$$\frac{d((\mathrm{C8:pC3}))}{dt} = \mathrm{k(5)\times C8\times pC3 - k\_(5)\times(C8:pC3) - kc(5)\times(C8:pC3)} \quad (42)$$

$$\frac{d(\mathrm{C3})}{dt} = \mathrm{kc(5)\times(C8:pC3) - k(8)\times C3\times XIAP+ k\_(8)\times(XIAP:C3) - k(9)\times C3\times PARP+k\_(9)\times(C3:PARP)+kc(9)\times(C3:PARP) + kc(25)\times(Apop:pC3)} \quad (43)$$

$$\frac{d(\mathrm{XIAP})}{dt} = \mathrm{c4i}\times\frac{\mathrm{XIAP\_mRNA}}{\mathrm{Kxiap+XIAP\_mRNA}} - \mathrm{k(8)\times C3\times XIAP + k\_(8)\times(XIAP:C3)+kc(8)\times(XIAP:C3) - k(27)\times XIAP\times Apop+k\_(27)\times(Apop:XIAP) - k(28)\times XIAP\times Smac+ k\_(28)\times(Smac:XIAP)} \quad (44)$$

doi:10.6342/NTU201602117

$$\frac{d((\text{XIAP:C3}))}{dt} = \text{k(8)} \times \text{C3} \times \text{XIAP} - \text{k\_(8)} \times (\text{XIAP:C3}) - \text{kc(8)} \times (\text{XIAP:C3}) \quad (45)$$

$$\frac{d(\text{PARP})}{dt} = \text{k\_(9)} \times (\text{C3:PARP}) - \text{k(9)} \times \text{C3} \times \text{PARP} \quad (46)$$

$$\frac{d((\text{C3:PARP}))}{dt} = \text{k(9)} \times \text{C3} \times \text{PARP} - \text{k\_(9)} \times (\text{C3:PARP}) - \text{kc(9)} \times (\text{C3:PARP}) \quad (47)$$

$$\frac{d(\text{CPARP})}{dt} = \text{kc(9)} \times (\text{C3:PARP}) \quad (48)$$

$$\frac{d(\text{Bid})}{dt} = \text{k\_(10)} \times (\text{C8:Bid}) - \text{k(10)} \times \text{C8} \times \text{Bid} \quad (49)$$

$$\frac{d((\text{C8:Bid}))}{dt} = \text{k(10)} \times \text{C8} \times \text{Bid} - \text{k\_(10)} \times (\text{C8:Bid}) - \text{kc(10)} \times (\text{C8:Bid}) \quad (50)$$

$$\begin{aligned}\frac{d(\text{tBid})}{dt} = {} & \text{kc(10)} \times (\text{C8:Bid}) - \text{k(11)} \times \text{tBid} \times \text{Bcl2c} + \text{k\_(11)} \times (\text{Bcl2c:tBid}) \\ & - \text{k(12)} \times \text{tBid} \times \text{Bax} + \text{k\_(12)} \times (\text{tBid:Bax}) + \text{kc(12)} \times (\text{tBid:Bax})\end{aligned} \quad (51)$$

$$\frac{d(\text{Bcl2c})}{dt} = \text{bcla} \times \frac{\text{IKKa}}{\text{KBcl2c+IKKa}} - \text{k(11)} \times \text{tBid} \times \text{Bcl2c} + \text{k\_(11)} \times (\text{Bcl2c:tBid}) \quad (52)$$

$$\frac{d((\text{Bcl2c:tBid}))}{dt} = \text{k(11)} \times \text{tBid} \times \text{Bcl2c} - \text{k\_(11)} \times (\text{Bcl2c:tBid}) \quad (53)$$

$$\frac{d(\text{Bax})}{dt} = \text{k\_(12)} \times (\text{tBid:Bax}) - \text{k(12)} \times \text{tBid} \times \text{Bax} \quad (54)$$

$$\frac{d((\text{tBid:Bax}))}{dt} = \text{k(12)} \times \text{tBid} \times \text{Bax} - \text{k\_(12)} \times (\text{tBid:Bax}) - \text{kc(12)} \times (\text{tBid:Bax}) \quad (55)$$

$$\frac{d(\text{Bax*})}{dt} = \text{kc(12)} \times (\text{tBid:Bax}) - \text{k(13)} \times \text{Bax*} + \text{k\_(13)} \times \text{Baxm} \quad (56)$$

$$\begin{aligned}\frac{d(\text{Baxm})}{dt} = {} & \text{k(13)} \times \text{Bax*} - \text{k\_(13)} \times \text{Baxm} - \frac{1}{v} \times \text{k(14)} \times \text{Baxm} \times \text{Bcl2} \\ & + \text{k\_(14)} \times (\text{Baxm:Bcl2}) - \frac{1}{v} \times 2 \times \text{k(15)} \times \text{Baxm}^2 + 2 \times \text{k\_(15)} \times \text{Bax2}\end{aligned} \quad (57)$$

$$\begin{aligned}\frac{d(\text{Bcl2})}{dt} = {} & \text{k\_(14)} \times (\text{Baxm:Bcl2}) - \frac{1}{v} \times \text{k(14)} \times \text{Baxm} \times \text{Bcl2} \\ & - \frac{1}{v} \times \text{k(16)} \times \text{Bcl2} \times \text{Bax2} + \text{k\_(16)} \times (\text{Bax2:Bcl2}) \\ & - \frac{1}{v} \times \text{k(18)} \times \text{Bcl2} \times \text{Bax4} + \text{k\_(18)} \times (\text{Bax4:Bcl2})\end{aligned} \quad (58)$$

$$\frac{d((\text{Baxm:Bcl2}))}{dt} = \frac{1}{v} \times \text{k(14)} \times \text{Baxm} \times \text{Bcl2} - \text{k\_(14)} \times (\text{Baxm:Bcl2}) \quad (59)$$

doi:10.6342/NTU201602117

$$\frac{d(\text{Bax2})}{dt} = \frac{1}{v}\times \text{k(15)}\times \text{Baxm}^2 - \text{k\_(15)}\times \text{Bax2} - \frac{1}{v}\times \text{k(16)}\times \text{Bcl2}\times \text{Bax2} + \text{k\_(16)}\times \text{(Bax2:Bcl2)} - \frac{2}{v}\times \text{k(17)}\times \text{Bax2}^2 + 2\times \text{k\_(17)}\times \text{Bax4} \tag{60}$$

$$\frac{d(\text{(Bax2:Bcl2)})}{dt} = \frac{1}{v}\times \text{k(16)}\times \text{Bcl2}\times \text{Bax2} - \text{k\_(16)}\times \text{(Bax2:Bcl2)} \tag{61}$$

$$\frac{d(\text{Bax4})}{dt} = \frac{1}{v}\times \text{k(17)}\times \text{Bax2}^2 - \text{k\_(17)}\times \text{Bax4} - \frac{1}{v}\times \text{k(18)}\times \text{Bcl2}\times \text{Bax4} + \text{k\_(18)}\times \text{(Bax4:Bcl2)} - \frac{1}{v}\times \text{k(19)}\times \text{M}\times \text{Bax4} + \text{k\_(19)}\times \text{(Bax4:M)} \tag{62}$$

$$\frac{d(\text{(Bax4:Bcl2)})}{dt} = \frac{1}{v}\times \text{k(18)}\times \text{Bcl2}\times \text{Bax4} - \text{k\_(18)}\times \text{(Bax4:Bcl2)} \tag{63}$$

$$\frac{d(\text{M})}{dt} = \text{k\_(19)}\times \text{(Bax4:M)} - \frac{1}{v}\times \text{k(19)}\times \text{M}\times \text{Bax4} \tag{64}$$

$$\frac{d(\text{(Bax4:M)})}{dt} = \frac{1}{v}\times \text{k(19)}\times \text{M}\times \text{Bax4} - \text{k\_(19)}\times \text{(Bax4:M)} - \text{kc(19)}\times \text{(Bax4:M)} \tag{65}$$

$$\frac{d(\text{M*})}{dt} = \text{kc(19)}\times \text{(Bax4:M)} - \frac{1}{v}\times \text{k(20)}\times \text{M*}\times \text{CytoCm} + \text{k\_(20)}\times \text{(M*:CytoCm)} + \text{kc(20)}\times \text{(M*:CytoCm)} - \frac{1}{v}\times \text{k(21)}\times \text{M*}\times \text{Smacm} + \text{k\_(21)}\times \text{(M*:Smacm)} + \text{kc(21)}\times \text{(M*:Smacm)} \tag{66}$$

$$\frac{d(\text{CytoCm})}{dt} = \text{k\_(20)}\times \text{(M*:CytoCm)} - \frac{1}{v}\times \text{k(20)}\times \text{M*}\times \text{CytoCm} \tag{67}$$

$$\frac{d(\text{(M*:CytoCm)})}{dt} = \frac{1}{v}\times \text{k(20)}\times \text{M*}\times \text{CytoCm} - \text{k\_(20)}\times \text{(M*:CytoCm)} - \text{kc(20)}\times \text{(M*:CytoCm)} \tag{68}$$

$$\frac{d(\text{CytoCr})}{dt} = \text{kc(20)}\times \text{(M*:CytoCm)} - \text{k(22)}\times \text{CytoCr} + \text{k\_(22)}\times \text{CytoC} \tag{69}$$

$$\frac{d(\text{Smacm})}{dt} = \text{k\_(21)}\times \text{(M*:Smacm)} - \frac{1}{v}\times \text{k(21)}\times \text{M*}\times \text{Smacm} \tag{70}$$

$$\frac{d(\text{(M*:Smacm)})}{dt} = \frac{1}{v}\times \text{k(21)}\times \text{M*}\times \text{Smacm} - \text{k\_(21)}\times \text{(M*:Smacm)} - \text{kc(21)}\times \text{(M*:Smacm)} \tag{71}$$

$$\frac{d(\text{Smacr})}{dt} = \text{kc(21)}\times \text{(M*:Smacm)} - \text{k(26)}\times \text{Smacr} + \text{k\_(26)}\times \text{Smac} \tag{72}$$

doi:10.6342/NTU201602117

$$\frac{d(\text{CytoC})}{dt} = \text{k(22)} \times \text{CytoCr} - \text{k\_(22)} \times \text{CytoC} - \text{k(23)} \times \text{CytoC} \times \text{Apaf} + \text{k\_(23)} \times (\text{Apaf:CytoC}) + \text{kc(23)} \times (\text{Apaf:CytoC}) \quad (73)$$

$$\frac{d(\text{Apaf})}{dt} = \text{k\_(23)} \times (\text{Apaf:CytoC}) - \text{k(23)} \times \text{CytoC} \times \text{Apaf} \quad (74)$$

$$\frac{d(\text{Apaf:CytoC})}{dt} = \text{k(23)} \times \text{CytoC} \times \text{Apaf} - \text{k\_(23)} \times (\text{Apaf:CytoC}) - \text{kc(23)} \times (\text{Apaf:CytoC}) \quad (75)$$

$$\frac{d(\text{Apaf*})}{dt} = \text{kc(23)} \times (\text{Apaf:CytoC}) - \text{k(24)} \times \text{Apaf*} \times \text{pC9} + \text{k\_(24)} \times \text{Apop} \quad (76)$$

$$\frac{d(\text{pC9})}{dt} = \text{k\_(24)} \times \text{Apop} - \text{k(24)} \times \text{Apaf*} \times \text{pC9} \quad (77)$$

$$\frac{d(\text{Apop})}{dt} = \text{k(24)} \times \text{Apaf*} \times \text{pC9} - \text{k\_(24)} \times \text{Apop} - \text{k(25)} \times \text{pC3} \times \text{Apop} + \text{k\_(25)} \times (\text{Apop:pC3}) + \text{kc(25)} \times (\text{Apop:pC3}) - \text{k(27)} \times \text{XIAP} \times \text{Apop} + \text{k\_(27)} \times (\text{Apop:XIAP}) \quad (78)$$

$$\frac{d((\text{Apop:pC3}))}{dt} = \text{k(25)} \times \text{pC3} \times \text{Apop} - \text{k\_(25)} \times (\text{Apop:pC3}) - \text{kc(25)} \times (\text{Apop:pC3}) \quad (79)$$

$$\frac{d(\text{Smac})}{dt} = \text{k(26)} \times \text{Smacr} - \text{k\_(26)} \times \text{Smac} - \text{k(28)} \times \text{XIAP} \times \text{Smac} + \text{k\_(28)} \times (\text{Smac:XIAP}) \quad (80)$$

$$\frac{d((\text{Apop:XIAP}))}{dt} = \text{k(27)} \times \text{XIAP} \times \text{Apop} - \text{k\_(27)} \times (\text{Apop:XIAP}) \quad (81)$$

$$\frac{d((\text{Smac:XIAP}))}{dt} = \text{k(28)} \times \text{XIAP} \times \text{Smac} - \text{k\_(28)} \times (\text{Smac:XIAP}) \quad (82)$$

$$\frac{d(\text{C3\_Ub})}{dt} = \text{kc(8)} \times (\text{XIAP:C3}) \quad (83)$$

From Albeck et. al.'s study it is shown that the effector caspase cleavage has a switch-like behavior, which means the amount of cleaved effector caspases increase dramatically at some time after the stimulation of TRAIL ligand. Besides, the lag time

doi:10.6342/NTU201602117

between TRAIL ligand binding to caspase activation in each cell are found highly variable. The lag time varies from one to several hours, and the switching time interval was found to be relatively invariant, around 30 min.

2.3 Combined model of TNFα-induced NF-κB signaling transduction model and extrinsic apoptosis reaction model

Based on the TNFα-induced NF-κB signaling transduction model and extrinsic apoptosis reaction model we construct a complete mathematical model. According to Yuan et al.[5], upon binding to TNFα, the cytoplasmic death domain of trimerized TNFR1 recruits proteins of complex I and the subsequent disassembled complex I proteins lead to the formation of cytosolic complex IIa proteins. So in the combined model we simplify the formation of complex IIa, such that the amount of complex IIa is in proportion to the amount active TNFR1 (as seen in Eq 33). To account the FADD activity in complex IIa, which is not available from the Allbeck's proposed model [17], we assumed that the Caspase-8 catalytic activity of FADD would be the same in DISC (formed from active TRAIL receptor) as that in complex IIa (recruited from active TNFR1) (as seen in Eq 38).

Translocation of NF-κB to nucleus lead to the gene expression of baculoviral IAP repeat-containing 2 (c-IAP1), baculoviral IAP repeat-containing 3 (c-IAP2), baculoviral

doi:10.6342/NTU201602117

IAP repeat-containing 4 (XIAP) and FLIP, among others [1]. So here we simplified the model by combining the expression of c-IAP1, c-IAP2, XIAP with one component called XIAP, to represent the NF-κB dependent pro-survival activity, which inhibits Caspase-3 activation directly or indirectly (via decreasing the formation of apoptosome). The simplification is listed in Eq 43. The interaction and functions of XIAP and FLIP follow the model of Allbeck et al [11, 17]. Here, we further assume that the transcription efficiency of XIAP and FLIP are the same in our model to simplify the NF-κB dependent prosurvival effect to inhibit apoptosis (as seen in Eqs 30, 31, 34 and 44).

The NF-κB-independent activation of IKKβ can phosphorylate BH3-only protein (BAD) and further decrease the inhibition of Bcl-XL (one protein of Bcl2 protein family) [6]. Bcl-XL in cytoplasm is combined with BAD proteins, and remains inactive form. When BAD protein is phosphorylated via IKKβ, Bcl-XL will be free from binding, for pro-survival activity. This NF-κB-independent pathway is not included in both the Allbeck and Tay et al.'s models. To describe the comprehensive regulation of TNFα mediated pro-survival and apoptosis effects, we included the NF-κB-independent pathway into our model. We assume that cytoplasm Bcl-2 (Bcl-2c) represents the target anti-apoptotic proteins regulated by TNFα mediated NF-κB-independent pro-survival pathway, and the activation of IKK via complex I increases the free Bcl-2c, which further decrease the activation of tBID proteins (as seen in Eqs 52 and 53). Our final

doi:10.6342/NTU201602117

model comprises 78 species and 112 parameters. Parameters values are as listed in Table. 5. Abbreviation of ODE components are listed in Table. 6. For the newly added and modified processes, their parameters are C4iflip & Kflip (parameters involving the translation rate of FLIP protein), c4i & Kxiap (parameters involving the translation rate of XIAP protein), kbcla &KBcl2c (parameters involving the activation rate of Bcl2c mediated by IKK), C4rac & C5rac (parameters involving TNFR1 mediated complex IIa activation), and kcDEG37(3) (degradation rate of active Caspase). The process to choose and calibrate these newly added parameters are included in Chapter 3.

doi:10.6342/NTU201602117

Chapter 3 Model validation using dynamics data from published studies

3.1 Calibration of Caspase-3 activity under the condition of cell lines with WT, IKKβ −/−, RelA −/−

We explored the active form of Caspase-3 as the surrogate of apoptotic dynamics. This protease has been implicated as an “effector” caspase associated with the initiation of the “death cascade” and is therefore an important marker of the cell’s apoptotic activity [6]. According to Yan et al.[6], they measured the Caspase-3 activity in response to TNFα (5 ng/ml) stimulation over 9 hours by immunoblotting the cleavage of Caspase-3 substrate PARP in (1) wild type MEF cells (2) IKKβ −/− MEF cells, (3) RelA −/− MEF cells transfected with control siRNA (siCtrl), and (4) RelA −/− MEF cells transfected siRNA against cRel (sicRel), respectively (Fig. 7A). First, we used the experimental data of Caspase-3 activity of IKKβ −/− MEF cells in response to TNFα (5 ng/ml) (Fig. 7A) to choose the proper parameters value of C4rac, C5rac and kcDEG37(3). TNFR1 expression on these fibroblast cell lines is relatively high, and we assume the averaged numbers of TNFR1 per cell as 3000 copies/cell in this simulation.

doi:10.6342/NTU201602117

The σ and μ parameters of log-normal distribution are set to $\sqrt{2}$ and -1 following the setting of Tay et al. [9]. Both the NF-κB dependent pro-survival and NF-κB independent pro-survival pathways are inhibited in IKKβ −/− MEF cells, and so we set the parameter i1 involving translocation rate of NF-κB from cytoplasm to nucleus to 0, and the parameter kbcla involving IKK mediated activation rate of Bcl-2c to 0.00001 for further simulation. Since the experimental measurement of Caspase-3 activity (Fig. 7A) is based on a population of cells, we repeated the simulation for 100 times with randomly picked TNFR1 amount which follows the log normal distribution, and obtained the average Caspapse-3 dynamics for model fitting. We chose the parameters value of C4rac, C5rac and kcDEG37 as 0.00001, 0.00005 and 0.0004, and the corresponding simulation results that Td (time to half of the maximal Caspase-3 activity) is around 3 hours and Tmax (time to maximal Caspase-3 activity) is around 5 hours (Fig. 5).

Second, we used the experimental data of Caspase-3 activity in RelA −/− MEF cells in response to TNFα (5 ng/ml) (Fig. 7A) to choose the proper parameters value of kbcla and KBcl2c. Since only the NF-κB dependent pro-survival pathway is inhibited in the RelA −/− MEF cells, we set the parameter i1 involving translocation rate of NF-κB from cytoplasm to nucleus to 0 for simulation. We also used the averaged Caspase-3 activity out of 100 times simulation with randomly chosen TNFR1 copy numbers per

doi:10.6342/NTU201602117

cell following the log normal distribution for simulation. We chose the parameters value of kbcla and KBcl2c as 0.45 and 30, and the corresponding simulation results indicated that Td is around 5 hours, Tmax is about 8-9 hours, and maximal Caspase-3 activity is about 70% of that of IKKβ −/− MEF cells.

Finally, we used the experimental data of Caspase-3 activity in wild type MEF cells in response to TNFα (5 ng/ml) (Fig. 7A) to choose the proper parameters value of C4iflip & Kflip and c4i & Kxiap. Because both the NF-κB dependent pro-survival and NF-κB independent pro-survival pathways are intact in wild type MEF cells, we set the parameter i1 involving translocation rate of NF-κB from cytoplasm to nucleus to 0.01 and kbcla / KBcl2c to 0.45/30. We chose the parameters value of C4iflip & Kflip and c4i & Kxiap as 0.3 & 800 and 63 & 80 , which is the value to fit the results that the Caspase-3 activity throughout 10 hours post TNFα stimulation is below 1% of maximal Caspase-3 of that of IKKβ −/− fibroblast cell lines (Fig.7B).

3.2 Calibration of Caspase-8 activity under the 10, 50, and 200 ng/ml TNFα

Caspase-8 is a member of the cysteine proteases and the activated Caspase-8 is known to propagate the apoptotic signal either by directly cleaving and activating

doi:10.6342/NTU201602117

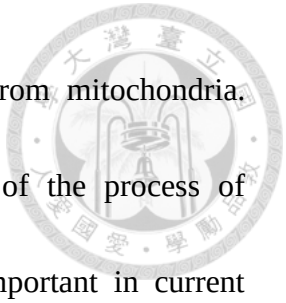

downstream caspases or leads to the release of Cytochrome c from mitochondria. Activation of Caspase-8 could be regarded as the "beginning" of the process of apoptosis [18] and calibration of Caspase-8 activity would be important in current modeling. In Fig. 8 which was adopted from the work of Fotin-Mleczek et al.[7], Caspase-8 activity was measured for over 400 minutes in the HeLa cell lines which are pre-incubated with cycloheximide (2.5 μg/ml) for 3 hours with TNFα 10 ng/ml, TNFα 10 ng/ml with co-stimulation of anti-TNF-R2 IgG, and TNFα 10 ng/ml with pre-stimulation of anti-TNF-R2 IgG. Anti-TNF-R2 IgG can induce depletion of TRAF2 and IAP proteins and accelerates TNFR1-dependent activation of Caspase-8.

A good calibration for the model would be direct measurement of different dosage of TNFα with detailed quantitative activation of Caspase-8. Unfortunately, it is not available in the literature yet. Since the effect of pre-stimulation or co-stimulation with anti-TNF-R2 IgG is in increased TNFR1-dependent activation of Caspase-8, we assumed that the Caspase-8 activity in response to the stimulation of TNFα 10 ng/ml with pre-stimulation or co-stimulation of anti-TNF-R2 IgG can be simulated with Caspase-8 activity in response to TNFα 50 ng/ ml and 200 ng/ml, respectively. The dynamic data from Fig. 9A could be used to validate our model in the respect of Caspase 8 activity under the stimulation of different TNFα concentration.

As HeLa cell line is known to have less TNFR1 expression [6], we assumed the

doi:10.6342/NTU201602117

average TNFR1 number as 150 copies/cell in this simulation, and all other parameters remain the same. Since the Caspase-8 activity is based on the expression of population of cells, we repeated the simulation for 100 times with random numbers of TNFR1 which follows the log normal distribution as proposed by Tay et al. The averaged Caspase-8 activity of simulation results during 400 minutes after the treatment of 10, 50, 200 ng/ml TNFα is included in Fig. 9, and in these results, the time to maximal Caspase-8 activity is around 4-6 hours, and higher maximal Caspase-8 activity is seen with higher TNFα stimulation. Our simulation results shared these similar properties with the experimental results, in Caspase-8 activity of HeLa cells after the treatment of TNFα 10 ng/ml, TNFα ng/ml with co-stimulation of anti-TNF-R2 IgG, and TNFα 10 ng/ml with prestimulation of anti-TNF-R2 IgG.

3.3 Calibration of apoptosis under different concentration of TNFα of wide type and I-kBα mutant cell lines

Cell viability is one direct measurement for the effect of apoptosis. Experimental observation on the cell viability under different TNFα concentrations (0.1, 1, 10, 100, 1000 ng/ml) was reported in the wide type and I-kBα mutant HT1080 fibrosarcoma cell

doi:10.6342/NTU201602117

lines, after 48 hrs of TNFα stimulation [19] (Fig. 10). TNFR1 expression of the SK-N-AS (neuroblastoma cell line) is thought to be less than MEF cells (fibroblast cell line) and the HT1080 fibrosarcoma cell lines is similar to the SK-N-AS cells, so we chose average number of membrane TNFR1 as 1000 copies/cell for the simulations, with all other parameters kept the same. We chose the threshold of Caspase-3 activity leading to cell apoptosis as 4×10^5 copies/cell, and repeated 200 simulations to calculate the probability of apoptosis. For the condition of the I-kBα mutant cell line, the translocation rate of NF-κB from cytoplasm to nucleus was set to 0. The simulated apoptosis probability under the treatment of TNFα 0.1, 0.5, 1, 5, 10, 50, 100 ng/ml were 0%, 16%, 34%, 79%, 89% and 100%, respectively. For wide type cell line, the apoptosis probability under 0.1-100 ng/ml were all 0. The increase of apoptosis probability of I-kBα mutant cells from 10% to 90% was seen in our simulation, under 0.5 to 10 ng/ml TNFα treatment, which is similar with the experimental data [19] where the decrease of viability probability of I-kBα mutant cells was observed to drop from 90% to 10% under 0.5 to 10 ng/ml TNFα treatment (Fig. 11).

doi:10.6342/NTU201602117

3.4 Calibration of distribution of Td (Time to half of maximal Caspase-3 activity) under the treatment of TNFα: 100 ng/ml and 2.5 μg/ml cycloheximide

Time to half of maximal Caspase-3 activity (Td) is one usual efficiency measurement of apoptosis in response to various stimuli. According to Allbeck et al., [17] the Td in HeLa cell lines under the treatment of various concentration of TRAIL ligands (2 ng/ml to 1000ng/ml) have the normal distribution with coefficient of variation within the range of 15~26%. However, it was observed that the Td in Hela cell lines under TNFα 100 ng/ml have higher coefficient of variation of 42% [17]. Their model could not repeat the phenomenon well. We tried to use our current model to simulate the distribution of Td under the stimulation of TNFα 100 ng/ml.

To simulate the experimental results, we used the mean TNFR numbers of 150 copies/cell to represent the HeLa cell lines, set the translocation rate of NF-κB from cytoplasm to nucleus to 0 to mimic the effect of cycloheximide. Repeated simulation with random TNFR numbers which followed the log normal distribution for 200 times was done to get the data of Td. Our result showed that the mean Td, standard deviation of Td, and coefficient of variation were 452 minutes, 188 minutes, 41.52%, which were well correlated to the Allbeck et al.'s data [17] (Fig. 12 and 13).

doi:10.6342/NTU201602117

3.5 Roburstness of the model: sensitivity analysis of the parameters

Parametric sensitivity analysis (PSA) is one useful tool in computational systems biology to study the parametric dependence of the targeted biological pathway and to elucidate important cellular processes that regulate the dynamics. Small change in the sensitive parameters may cause a big perturbation in the dynamic of the system. PSA could help us to find the key components and reactions of the network/model by identifying where such small changes might be, and how they could cause large change in the consequences.

A standard PSA could be performed by calculating the sensitivity at time t ($S_{ij}(t)$), which is defined as the ratio of the difference between the original and the new outputs signal i ($\Delta X_i := X_i - X_{i\_old}$) to the variation of (input) parameter j ($\Delta P_j = P_j - P_{j\_old}$), with normalization to their original values (X_i and P_j).

$$S_{ij}(t) = \frac{P_j}{X_i} \times \frac{\Delta X_i}{\Delta P_j} = \frac{P_j}{X_i} \times \frac{X_i - X_{i\_old}}{P_j - P_{j\_old}} \qquad (84)$$

In the current study, we increase ΔP_j by +1% of the original value, and use it to obtain the ΔX_i. We then sum absolute values, avoiding cancellation of positive and negative

doi:10.6342/NTU201602117

sensitivities, and calculate the time-averaged sensitivities S_{ij} according to:

$$S_{ij} = \int |S_{ij}(t)|\, dt \tag{85}$$

We categorized all parameters into 6 groups according to the pathways they are involved: TNFα-TNFR1 interaction, complex I mediated IKK activation, complex II mediated Caspase 8 activation, IKK mediated cytosol Bcl-2c upregulation and TNFα mediated extrinsic apoptosis pathway. In the current study, PSA was performed under TNFα 100 and 0.5 ng/ml conditions, and the results are included in Fig. 14 and 15, respectively.

To see if there are systematic variance among different groups of parameters in their sensitivity, we performed the analysis of variance (ANOVA) test, and it revealed non-significant difference (p=0.09) of the mean sensitivity between any 2 of the 6 groups under TNFα 100 ng/ml, but significant difference ($p= 8.8\times10^{-5}$) under TNFα 0.5 ng/ml (Tables 1 and 2).

To simplify the discussion and derive insights, we divide the parameters into 6 different groups according to the processes they are involved: (1) involving TNFα-TNFR1 interaction, (2) complex I mediated IKK activation, (3) complex II mediated Caspase-8 activation, (4) IKK mediated cytoplasm Bcl-2c up-regulation, (5)

doi:10.6342/NTU201602117

NF-κB-dependent pro-survival signal pathway, and (6) TNFα mediated extrinsic apoptosis pathway. The ratio of the averaged value of parameter sensitivity score under TNFα 0.5 ng/ml to TNFα 100 ng/ml among the six groups of parameters are 2.89, 73, 2, 12, 4 and 4 respectively. We can see that the group of parameters involving complex I mediated IKK activation and IKK mediated Bcl-2c up-regulation both have larger changes in parameter sensitivity under the stimulation of TNFα 0.5 ng/ml compared to TNFα 100 ng/ml. With this result, we proceed and further simulate the apoptosis probability of different cell lines with the inhibition of parameters involving these pathways under various TNFα stimulation.

3.6 Application of the Results of parametric sensitivity analysis

In order to evaluate the effect of higher fold change in parameter sensitivity under the stimulation of TNFα 0.5 ng/ml compared to TNFα 100 ng/ml, we choose the parameter i1 within the group of parameters involving NF-κB-dependent pro-survival signal pathway and parameter kbcla within the group of parameters involving IKK mediated Bcl-2c up-regulation as the target to inhibit pathway and simulate the apoptosis probability under the stimulation of different TNFα concentration and different cell lines (HeLa and MEF cells). The fold change of i1 and kbcla in parameter

doi:10.6342/NTU201602117

sensitivity score under the stimulation of TNFα 0.5 ng/ml compared to TNFα 100 ng/ml are 0.324 and 7.84, respectively. We set the kbcla to 1% of the original value, and i1 to 0 to represent the inhibition on IKK mediated Bcl-2c up-regulation and NF-κB-dependent pro-survival signal pathway. The average membrane TNFR1 numbers per cell of HeLa and MEF cells are set to 150 and 5000 copies/cell, respectively. The TNFR expression of MEF was reported to be 1000-10000 per cell. In order to enhance the contrast between HeLa and MEF cells in the performance, we picked a slightly higher value (5000) in the following simulation. We chose the threshold of Caspase-3 activity for cell apoptosis as 4×10^5, and 100 simulations were repeated to calculate the probability of apoptosis.

The results of apoptosis probability of HeLa and MEF cells under the inhibition of IKK mediated Bcl-2c up-regulation and NF-κB-dependent pro-survival signal pathway and stimulation of various TNFα concentrations are listed in Tables 3 and 4. When we inhibit the NF-κB-dependent pro-survival signal pathway, the apoptosis probability of both HeLa and MEF cells increased with the higher concentration of TNFα. The TNFα concentration required for 50% apoptosis probability is around 5-10 ng/ml for HeLa cells and 0.1-0.5 ng/ml for MEF cells, respectively (Table 4). When the IKK mediated Bcl-2c up-regulation pathway is inhibited, peak value of apoptosis probability can be found around TNFα 1 ng/ml for HeLa cells and TNFα 0.05 ng/ml for MEF cells (Table

doi:10.6342/NTU201602117

3).

The HeLa cells is derived from cervical cancer, and could be regarded as a representation of malignant cells. The MEF cells derived from fibroblast cells, and could be regarded as normal cells. In order to compare the apoptosis probability under various TNFα stimulations between HeLa and MEF cells, we developed a therapeutic index, which also reflects the extend of a treatment that kills more malignant cells, such as HeLa cells, and less normal cells, such as MEF cells, under a set of given treatment, as,

$$\text{Therapeutic Index}=\frac{1+100\times\text{Apoptosis probability of HeLa}}{1+100\times\text{Apoptosis probability of MEF}} \qquad (86)$$

Where a small basal value, equivalent to 1% in apoptosis probability, was added to both denominator and numerator, and this is to avoid problems arising from a zero denominator. Under the inhibition of NF-κB-dependent pro-survival signal pathway, the therapeutic index score increases with higher TNFα concentration, and the highest score equals to 1 (Table. 4). The result means that we always kill the same amount or more MEF cells than HeLa cells via TNFα stimulation when we inhibit the NF-κB-dependent pro-survival signal pathway. In contrast, for the inhibition of IKK mediated Bcl-2c up-regulation pathway, the therapeutic index score is higher than 1 around the

doi:10.6342/NTU201602117

stimulation of TNFα 0.5-100 ng/ml and the highest score value is 151 under the stimulation of TNFα 5 ng/ml (Table. 3). The result indicates that, although the apoptosis probability under the inhibition of IKK mediated Bcl-2c up-regulation pathway is less than 25%, more HeLa cells can be killed compared to MEF cells with TNFα 0.1-100 ng/ml treatment (Table 4).

When inhibition is targeted to the pathways which parameters have higher fold change in parameter sensitivity score under the stimulation of TNFα 0.5 ng/ml compared to TNFα 100 ng/ml, it can increase the therapeutic benefits by killing more malignant cells in TNFα mediated apoptosis. The inhibition of those parameters will make cells more sensitive to apoptosis under lower TNFα concentration. Membrane TNFR1 copies/number will augment the effect of TNFα concentration mediated apoptosis and expand the therapeutic index under various TNFα concentration.

doi:10.6342/NTU201602117

Chapter 4 Conclusion and future work

To the best of our knowledge, the current mathematical model is the first which combines the TNFα-induced NF-κB dependent and independent pro-survival signaling transduction pathways, and TNFα mediated extrinsic apoptosis pathway to comprehensively describe how TNFα triggers the cell to survive or death. Total 78 species and 112 parameters are included in our model. Twenty-seven species (Eqs 5-31) are involved in the TNFα mediated extrinsic apoptosis pathway and 51 species (Eqs 33-83) are involved in the TNFα-induced NF-κB dependent and independent pro-survival signaling transduction pathway.

Our model can fit well to the dynamic change of Caspase-3 activity in response to TNFα 5 ng/ml in the experimental results of wild type, IKKβ −/−, and RelA -/- MEF cell lines. As for Caspase-8 activity under various TNFα concentration, our simulation results showed similar property with the experimental results of Caspase-8 activity of HeLa cells after the treatment of TNFα 10 ng/ml, TNFα ng/ml with co-stimulation of anti-TNF-R2 IgG, and TNFα 10 ng/ml with pre-stimulation of anti-TNF-R2 IgG. The viability probability of HT1080 cell lines from experimental data is also correlated well to our simulation result. Our model can repeat the experimental results of Td distribution with simulation results of the mean Td: 452 minutes, standard deviation of

doi:10.6342/NTU201602117

Td: 188 minutes, and coefficient of variation: 41.52% under the stimulation of TNFα 100 ng/ml.

The parametric sensitivity analysis of the model helps us obtain fold changes in parameter sensitivities under the stimulation of TNFα 0.5 ng/ml compared to TNFα 100 ng/ml. We further studied effects of inhibition targeted to the pathways which parameters have higher fold change in parameter sensitivity score under the stimulation of TNFα 0.5 ng/ml compared to that of TNFα 100 ng/ml, and found that such inhibition can increase the therapeutic benefits through TNFα mediated apoptosis. In particular, under the inhibition of IKK mediated Bcl-2c up-regulation pathway, the therapeutic index score is higher than 1 around the stimulation of TNFα 0.5-100 ng/ml and the highest score is 151 under the stimulation of TNFα 5 ng/ml. The human physiological TNFα concentration was reported less than 5 ng/ml [20], and our simulation could imply that the drugs targeted on BAD-Bcl-2c activation, for example selective IKKβ inhibitor or Bcl-2 inhibitor, would have higher therapeutic benefit than the drugs directly targeted on the translocation rate of NF-κB from cytoplasm to nucleus.

Our results could further provide insights for existing drugs in treatment of cancers. For example, cycloheximide has been discovered for a long time, and it was once regarded as a potent drug for cancer treatment. Nowadays, the evidence of the therapeutic benefit of cycloheximide is still limited to cell line evidence level due to

doi:10.6342/NTU201602117

high toxicity in the human body. In contrast, the Bcl-2 inhibitors, such as ABT-199, emerges as a rising star for cancer treatment. There are several clinical studies supporting the treatment effect of ABT-199 [21-24].

The mathematical model of TNFα mediated apoptosis and pro-survival pathway is a novel and efficient approach to understand the TNFα-induced apoptosis and to find valuable target for clinical use. Future study should be aimed to directly validate the dynamics of Caspase-3 and Caspase-8 activation in response to stimulation of various TNFα concentrations through different cell lines and conditions. Model predicted therapeutic benefit under different TNFα stimulation also requires experimental evidence. More comprehensive sensitivity analysis and therapeutic index scores of parameters can also be performed to further find the potential therapeutic targets for clinical investigations.

doi:10.6342/NTU201602117

Reference:

1. Fuentes-Prior P, Salvesen GS: **The protein structures that shape caspase activity, specificity, activation and inhibition.** *The Biochemical journal* 2004, **384:**201-232.
2. Probst-Cousin S, Rickert CH, Schmid KW, Gullotta F: **Cell death mechanisms in multiple system atrophy.** *Journal of neuropathology and experimental neurology* 1998, **57:**814-821.
3. Elmore S: **Apoptosis: a review of programmed cell death.** *Toxicologic pathology* 2007, **35:**495-516.
4. Ouyang L, Shi Z, Zhao S, Wang FT, Zhou TT, Liu B, Bao JK: **Programmed cell death pathways in cancer: a review of apoptosis, autophagy and programmed necrosis.** *Cell proliferation* 2012, **45:**487-498.
5. Ofengeim D, Yuan J: **Regulation of RIP1 kinase signalling at the crossroads of inflammation and cell death.** *Nature reviews Molecular cell biology* 2013, **14:**727-736.
6. Yan J, Xiang J, Lin Y, Ma J, Zhang J, Zhang H, Sun J, Danial NN, Liu J, Lin A: **Inactivation of BAD by IKK inhibits TNFalpha-induced apoptosis independently of NF-kappaB activation.** *Cell* 2013, **152:**304-315.
7. Fotin-Mleczek M, Henkler F, Samel D, Reichwein M, Hausser A, Parmryd I, Scheurich P, Schmid JA, Wajant H: **Apoptotic crosstalk of TNF receptors: TNF-R2-induces depletion of TRAF2 and IAP proteins and accelerates TNF-R1-dependent activation of caspase-8.** *Journal of cell science* 2002, **115:**2757-2770.
8. Flusberg DA, Sorger PK: **Surviving apoptosis: life-death signaling in single cells.** *Trends in cell biology* 2015, **25:**446-458.
9. Tay S, Hughey JJ, Lee TK, Lipniacki T, Quake SR, Covert MW: **Single-cell NF-kappaB dynamics reveal digital activation and analogue information processing.** *Nature* 2010, **466:**267-271.
10. Pekalski J, Zuk PJ, Kochanczyk M, Junkin M, Kellogg R, Tay S, Lipniacki T: **Spontaneous NF-kappaB activation by autocrine TNFalpha signaling: a computational analysis.** *PloS one* 2013, **8:**e78887.
11. Albeck JG, Burke JM, Aldridge BB, Zhang M, Lauffenburger DA, Sorger PK: **Quantitative analysis of pathways controlling extrinsic apoptosis in single cells.** *Molecular cell* 2008, **30:**11-25.
12. O'Donnell MA, Ting AT: **NFkappaB and ubiquitination: partners in disarming RIPK1-mediated cell death.** *Immunologic research* 2012, **54:**214-226.

doi:10.6342/NTU201602117

13. Ting AT, Pimentel-Muinos FX, Seed B: **RIP mediates tumor necrosis factor receptor 1 activation of NF-kappaB but not Fas/APO-1-initiated apoptosis.** *EMBO J* 1996, **15:**6189-6196.
14. Ea CK, Deng L, Xia ZP, Pineda G, Chen ZJ: **Activation of IKK by TNFalpha requires site-specific ubiquitination of RIP1 and polyubiquitin binding by NEMO.** *Molecular cell* 2006, **22:**245-257.
15. O'Donnell MA, Legarda-Addison D, Skountzos P, Yeh WC, Ting AT: **Ubiquitination of RIP1 regulates an NF-kappaB-independent cell-death switch in TNF signaling.** *Curr Biol* 2007, **17:**418-424.
16. Mogilner A, Allard J, Wollman R: **Cell polarity: quantitative modeling as a tool in cell biology.** *Science* 2012, **336:**175-179.
17. Albeck JG, Burke JM, Spencer SL, Lauffenburger DA, Sorger PK: **Modeling a snap-action, variable-delay switch controlling extrinsic cell death.** *PLoS biology* 2008, **6:**2831-2852.
18. Kruidering M, Evan GI: **Caspase-8 in apoptosis: the beginning of "the end"?** *IUBMB life* 2000, **50:**85-90.
19. Micheau O, Tschopp J: **Induction of TNF receptor I-mediated apoptosis via two sequential signaling complexes.** *Cell* 2003, **114:**181-190.
20. Turner DA, Paszek P, Woodcock DJ, Nelson DE, Horton CA, Wang Y, Spiller DG, Rand DA, White MR, Harper CV: **Physiological levels of TNFalpha stimulation induce stochastic dynamics of NF-kappaB responses in single living cells.** *Journal of cell science* 2010, **123:**2834-2843.
21. Pan R, Hogdal LJ, Benito JM, Bucci D, Han L, Borthakur G, Cortes J, DeAngelo DJ, Debose L, Mu H, et al: **Selective BCL-2 inhibition by ABT-199 causes on-target cell death in acute myeloid leukemia.** *Cancer discovery* 2014, **4:**362-375.
22. Tam CS, Seymour JF, Roberts AW: **Progress in BCL2 inhibition for patients with chronic lymphocytic leukemia.** *Semin Oncol* 2016, **43:**274-279.
23. Jain N, O'Brien S: **Targeted therapies for CLL: Practical issues with the changing treatment paradigm.** *Blood Rev* 2016, **30:**233-244.
24. Roberts AW, Davids MS, Pagel JM, Kahl BS, Puvvada SD, Gerecitano JF, Kipps TJ, Anderson MA, Brown JR, Gressick L, et al: **Targeting BCL2 with Venetoclax in Relapsed Chronic Lymphocytic Leukemia.** *The New England journal of medicine* 2016, **374:**311-322.

doi:10.6342/NTU201602117

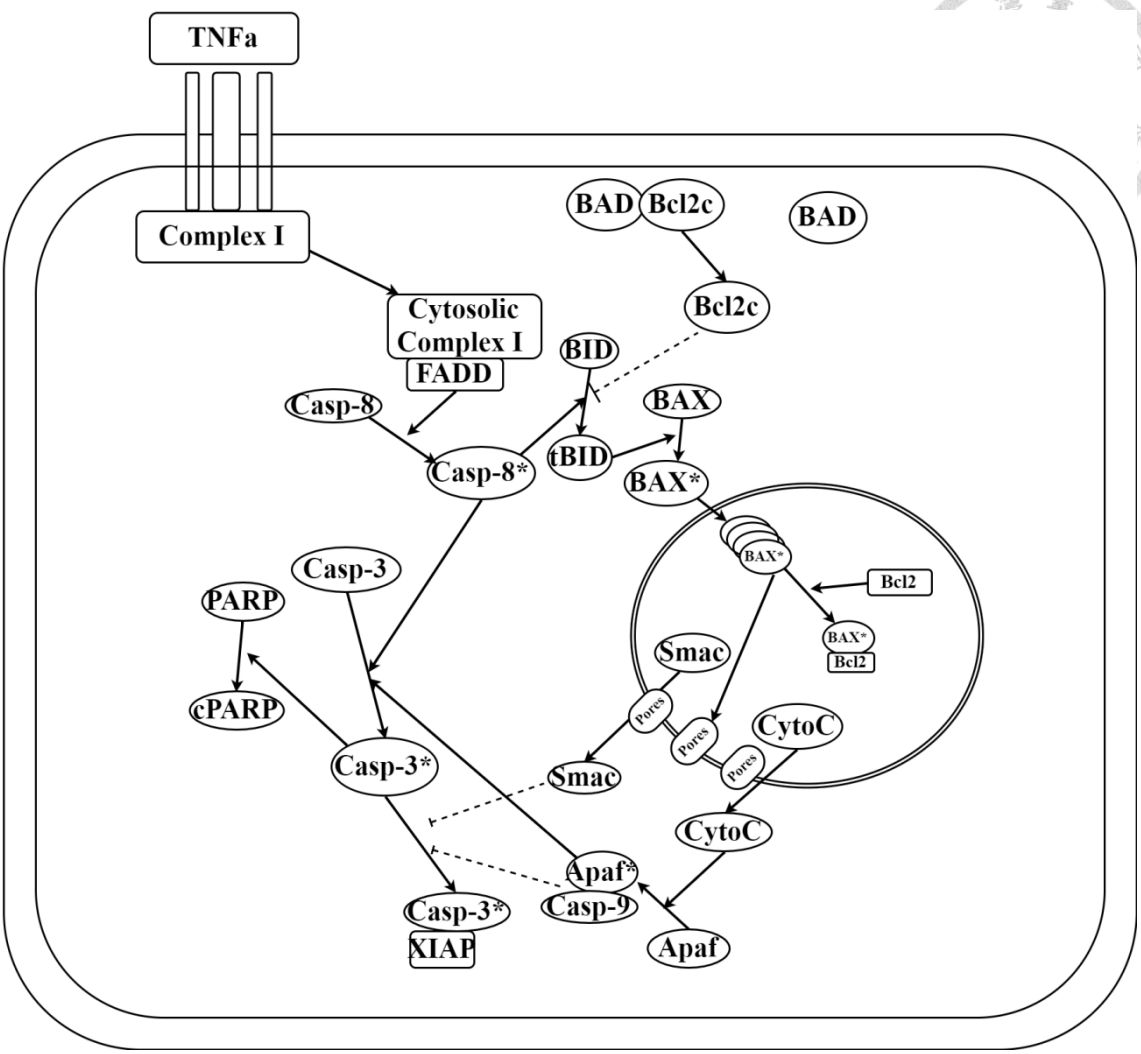

Fig. 1 TNFα mediated extrinsic apoptosis pathway included in the present work. Shown are processes taken on the cell membrane (outer boundary), cytoplasm (between two boundaries) and inside mitochondria (in the circular boundary). Arrows indicates protein state changing, relocation, or activation when it ends on another. Dashed lines indicates repression or inhibition.

doi:10.6342/NTU201602117

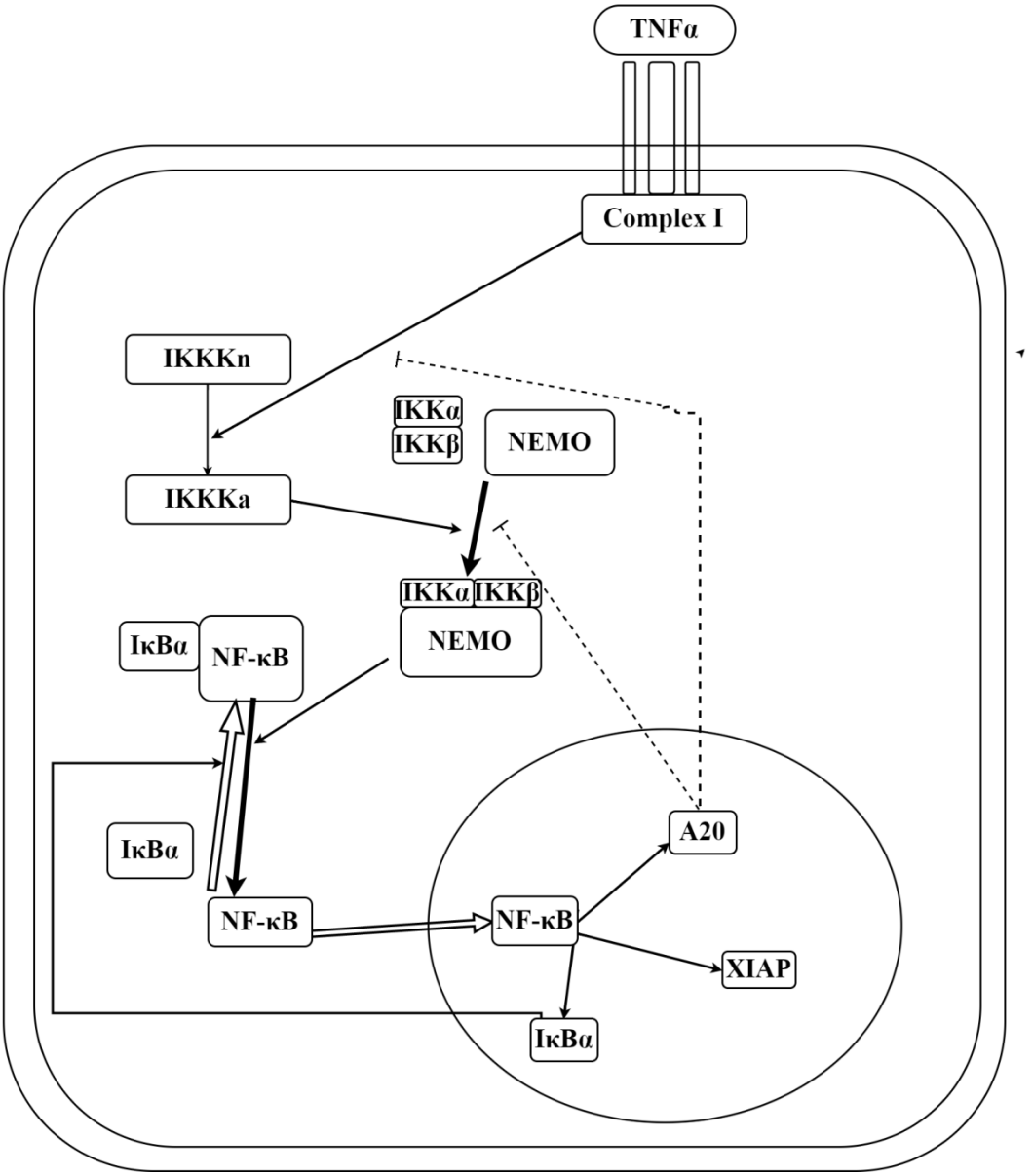

Fig. 2 TNFα mediated NF-κB activation pathways included in the present work. Shown are processes taken on the cell membrane (outer boundary), cytoplasm (between two boundaries) and inside nucleus (in the circular boundary). Arrows indicates protein state changing, relocation, or activation when it ends on another. Dashed lines indicates repression or inhibition.

doi:10.6342/NTU201602117

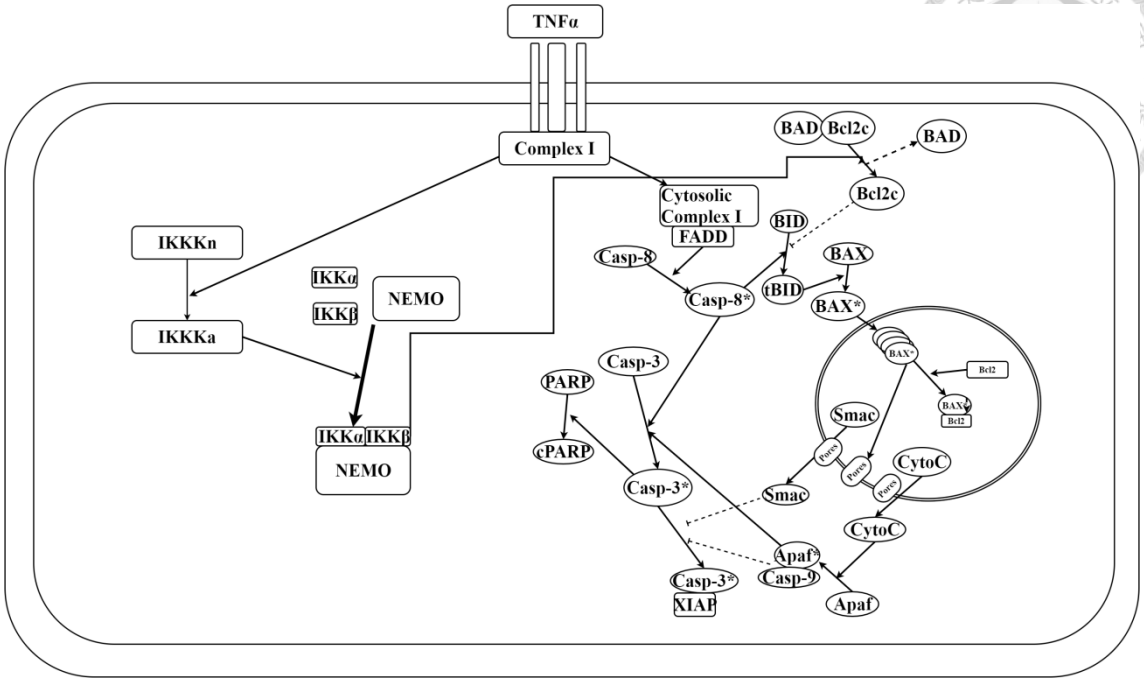

Fig. 3 TNFα mediated NF-κB-independent pro-survival pathways included in the present work. Other details are similar to those for Fig.1.

doi:10.6342/NTU201602117

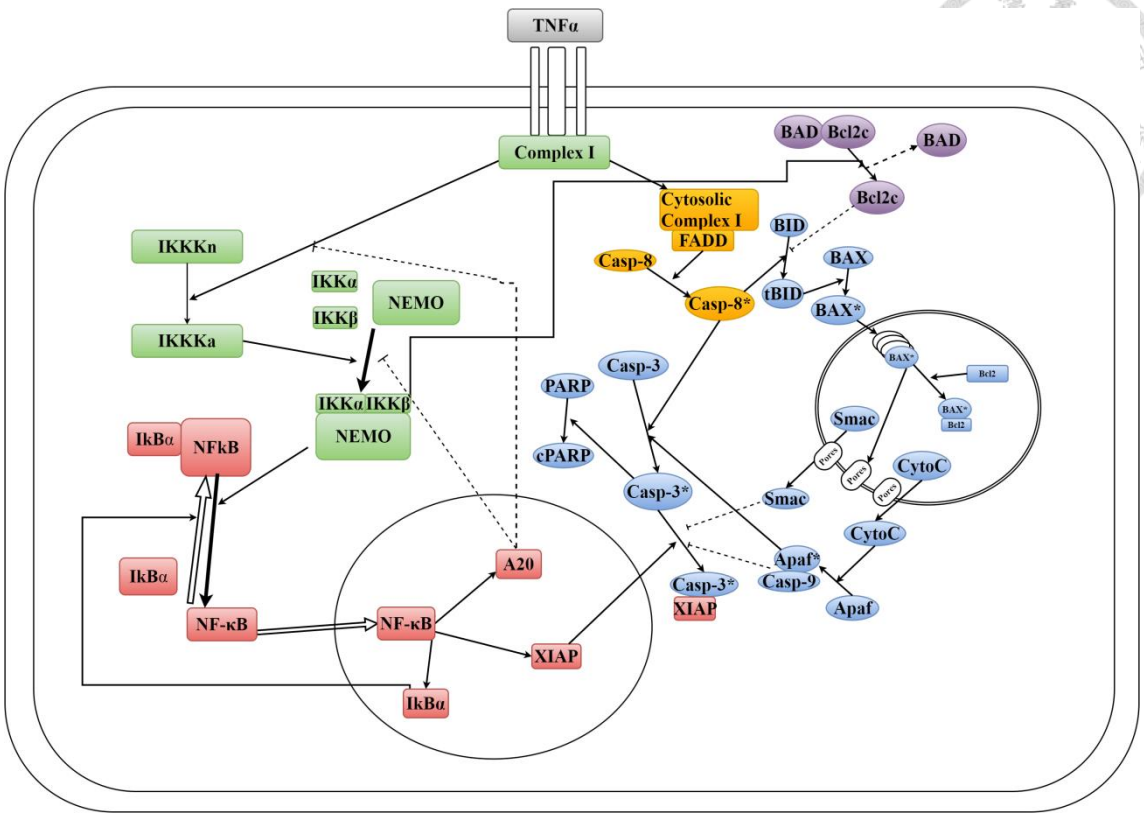

Fig. 4 The combination of TNFα mediated apoptosis and prosurvival pathways included in the present work. Other details are similar to those for Fig.1 and Fig. 2.

doi:10.6342/NTU201602117

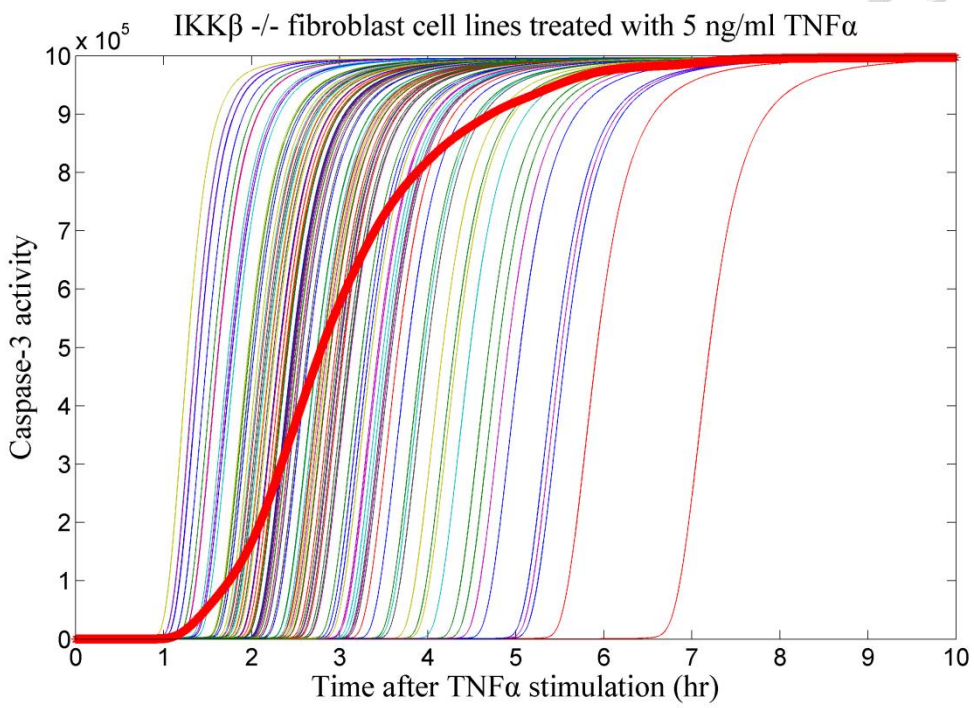

Fig. 5 Simulation results of IKKβ −/− fibroblast cell lines treated with 5 ng/ml TNFα. Thin colored lines are for each individual cell, simulated by a sampling for different copy numbers of membrane TNFR1 per cell, and the thick red line is for the population averaged activity. Simulation was performed with Eqs. 5-83 and parameters were set as those listed in Table 5.

doi:10.6342/NTU201602117

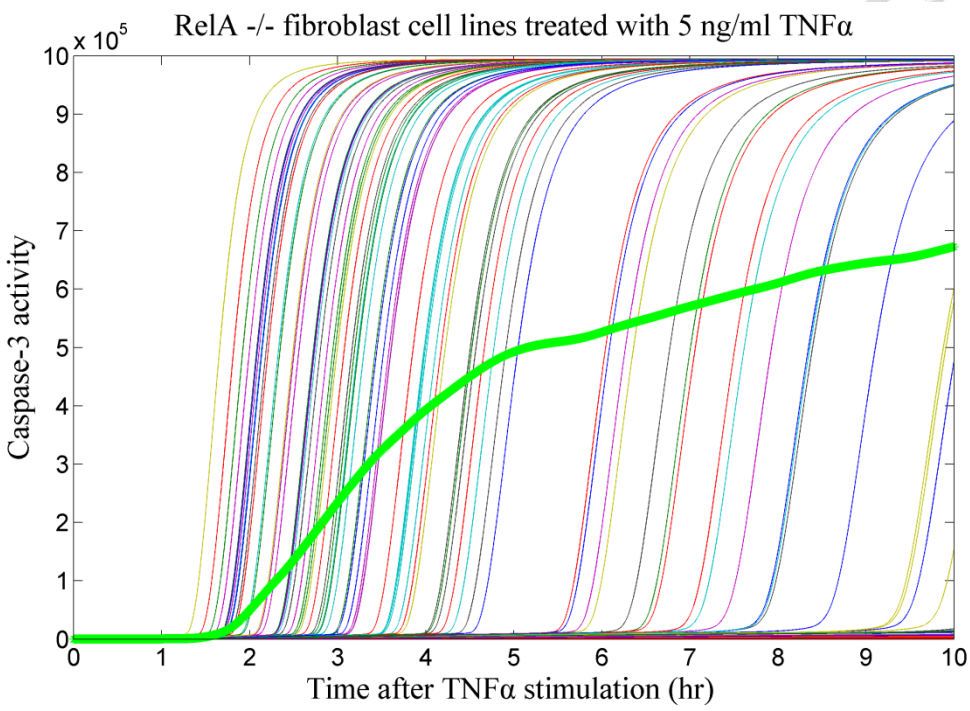

Fig. 6 Simulation results of RelA −/− fibroblast cell lines treated with 5 ng/ml TNFα. Thin colored lines are for each individual cell, simulated by a sampling for different numbers of membrane TNFR1 and the thick red line is for the population averaged activity. Simulation was performed with Eqs. 5-83 and parameters were set as those listed in Table. 5.

doi:10.6342/NTU201602117

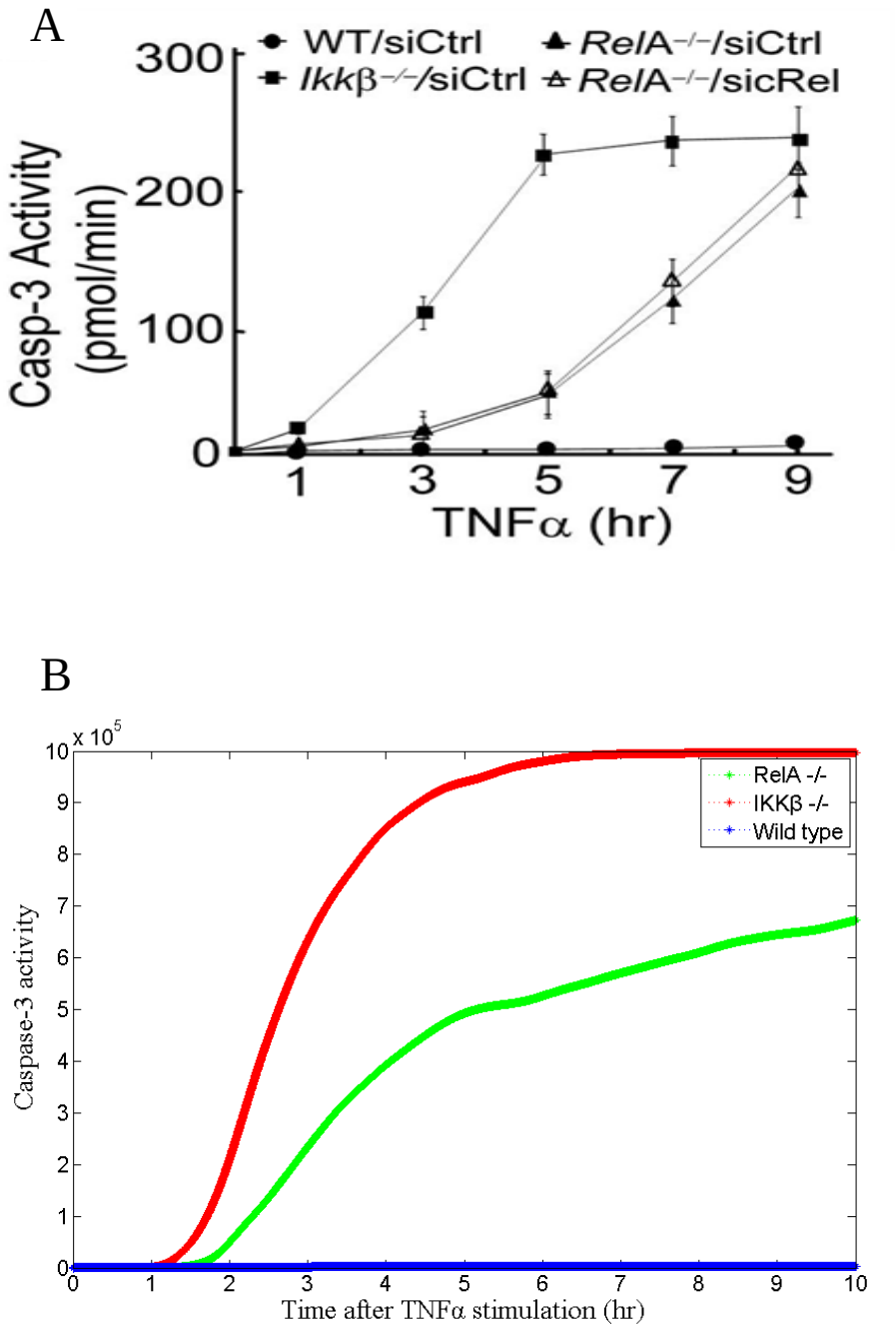

Fig. 7 A&B Comparison of experiment and simulation results for the Caspase-3 activities in fibroblasts treated with TNF- α (5 ng/ml). Shown in (A) are experimental results for IKKβ −/−, RelA −/− and Wild Type fibroblasts, adoped from Ref. [6], and in (B) are simulation result.

doi:10.6342/NTU201602117

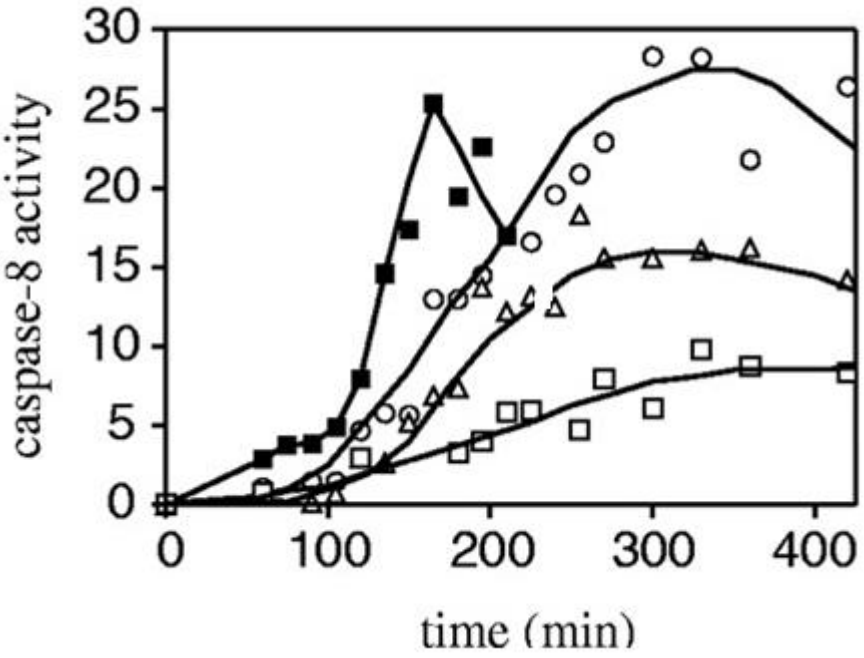

Fig. 8 Time-dependent Caspase-8 activity under different TNFα simulation. Experiments were performed with HeLa cells pre-incubated with cycloheximide (2.5 μg/ml) for 3 hours. Shown are results from treatment with TNFα 10 ng/ml TNF (□), TNFα 10 ng/ml with co-stimulation of anti-TNF-R2 IgG (Δ), and TNFα 10 ng/ml with pre-stimulation of anti-TNF-R2 IgG(o), respectively. Figure taken from Ref.[7]

doi:10.6342/NTU201602117

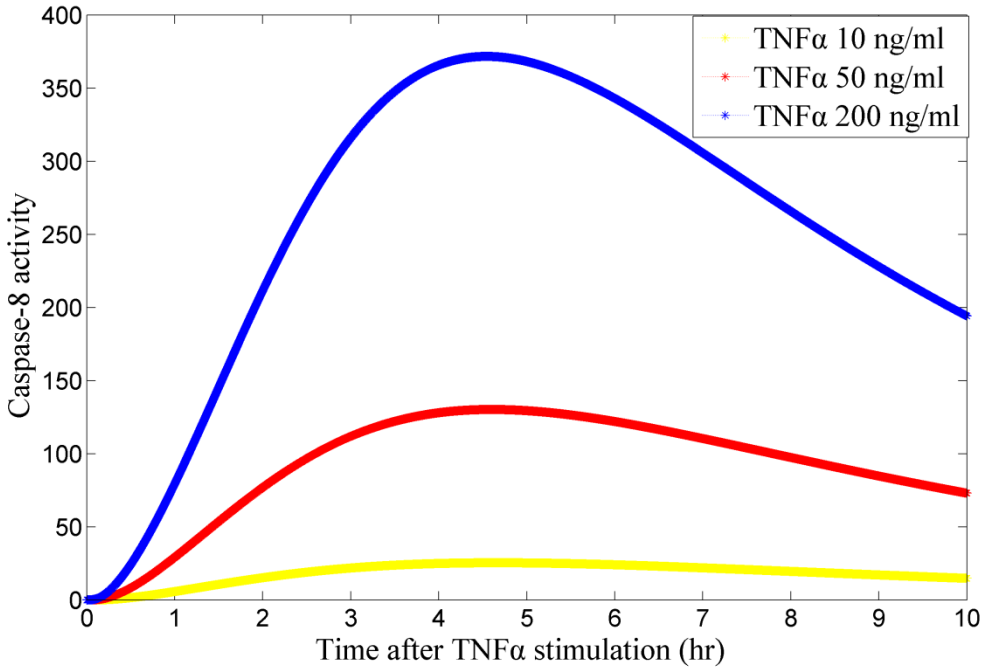

Fig. 9 Simulation results of Caspase-8 activity during 400 minutes after 10, 50, 200 ng/ml TNFα stimulation of HeLa cell line.

doi:10.6342/NTU201602117

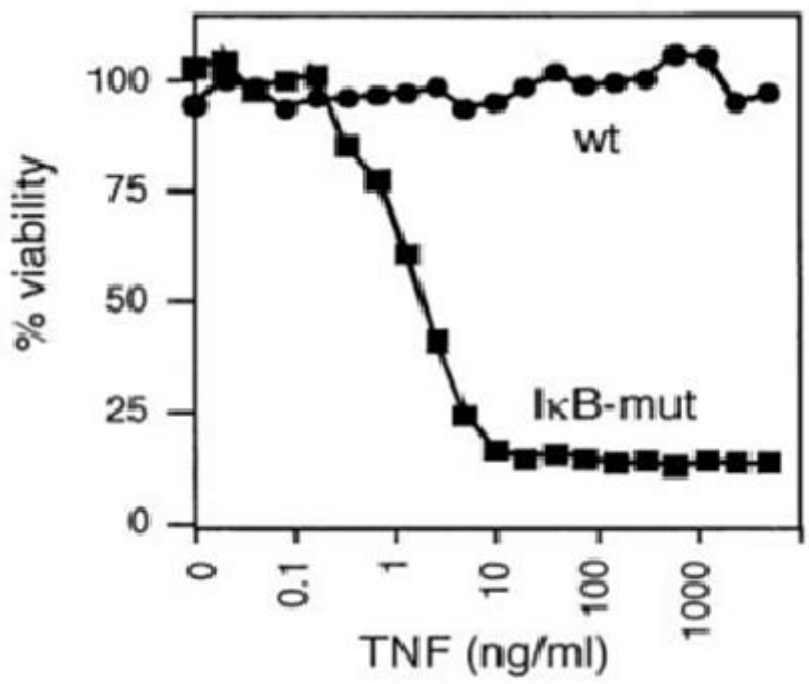

Fig. 10 Viability probability of wide type and I-kBa mut HT1080 fibrosarcoma cell lines treated with TNFα 0.1, 1, 10, 100, 1000 ng/ml. Figure taken from Ref. [19]

doi:10.6342/NTU201602117

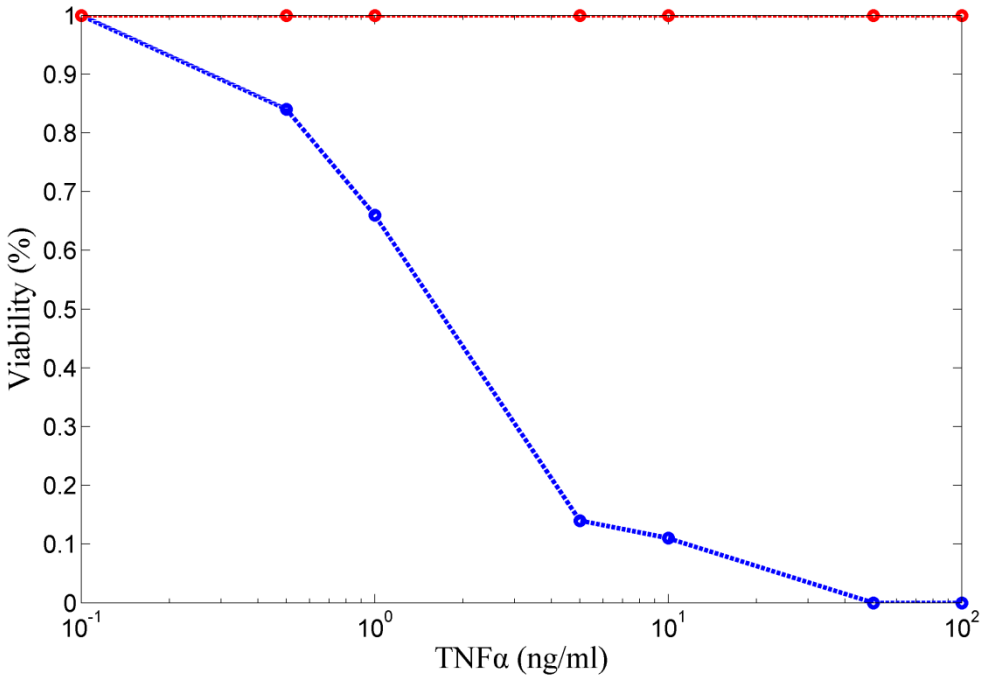

Fig. 11 Simulation result of viability probability under the treatment of TNFa 0.1, 0.5, 1, 5, 10, 50, 100 ng/ml.

doi:10.6342/NTU201602117

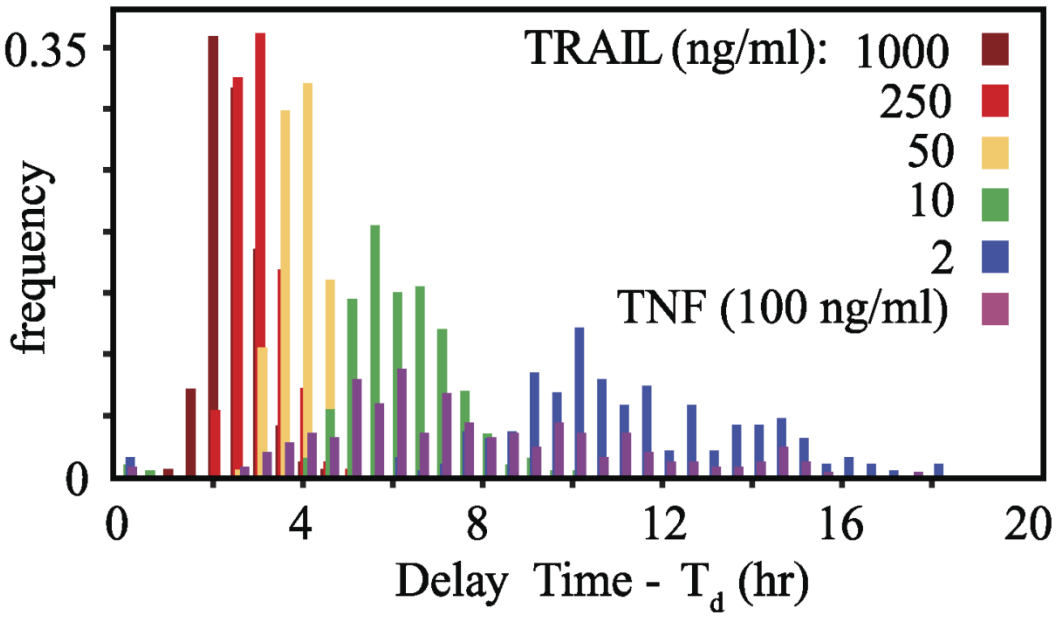

Fig. 12 Delay time of Caspase-3 maximal activity of HeLa cell line under 100 ng/ml. TNFα and 2, 10, 50, 250, 1000 ng/ml TRAIL ligands. Figure taken from Ref. [17].

doi:10.6342/NTU201602117

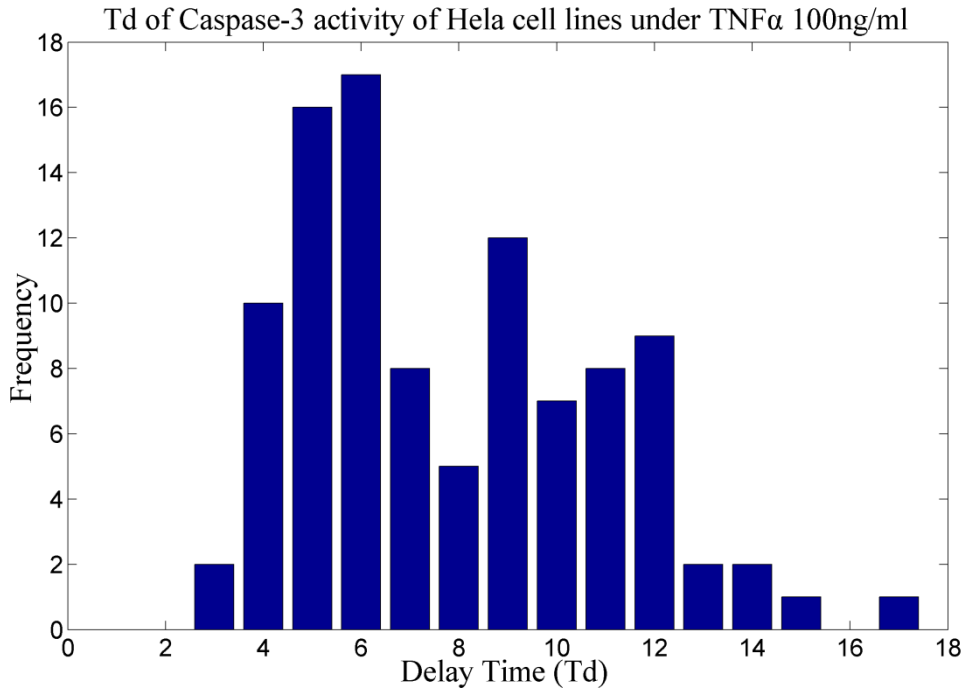

Fig. 13 Simulation results based on our model for the Td of Caspase-3 activity of HeLa cell lines treated with TNF α 100 ng/ml

doi:10.6342/NTU201602117

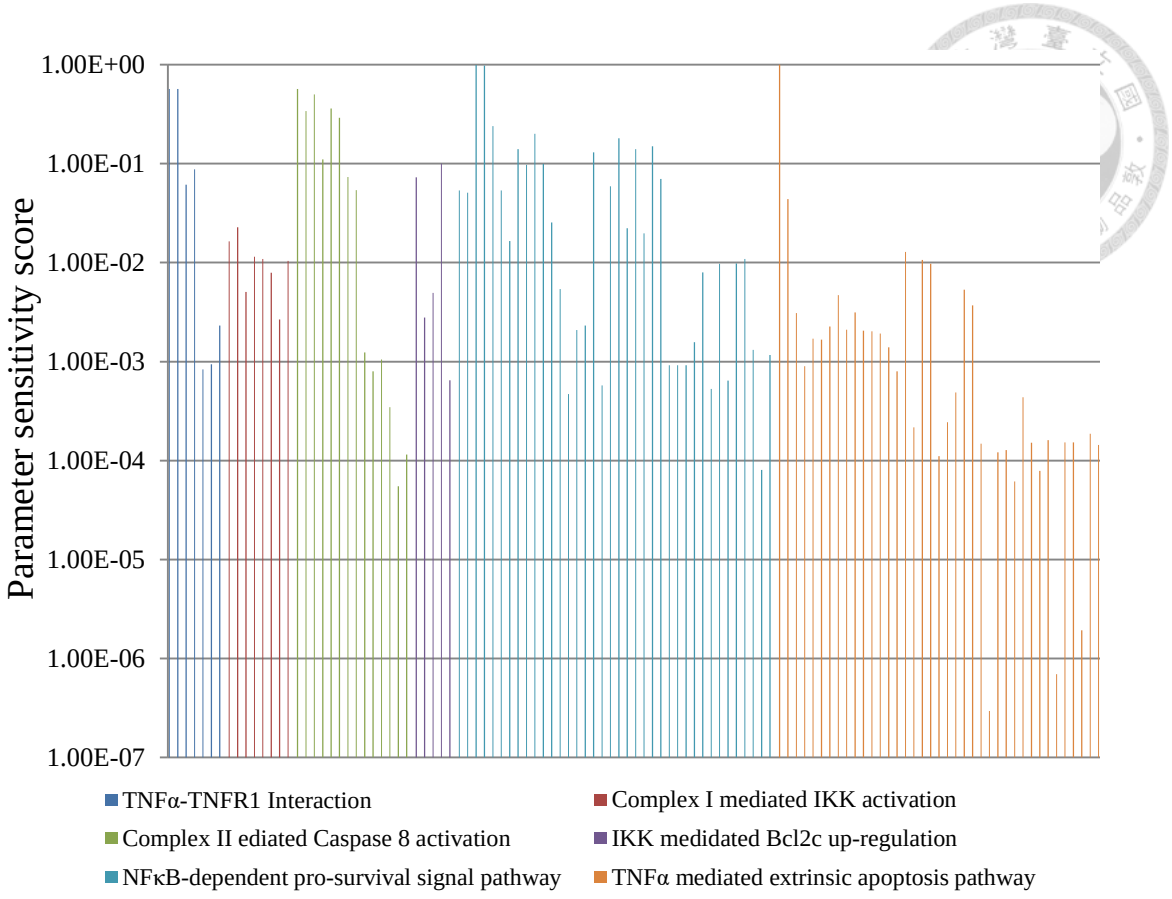

Fig. 14 Sensitivity analysis for parameters in the current model, performed in HeLa cell line setting under TNFα 100 ng/ml treatment.

doi:10.6342/NTU201602117

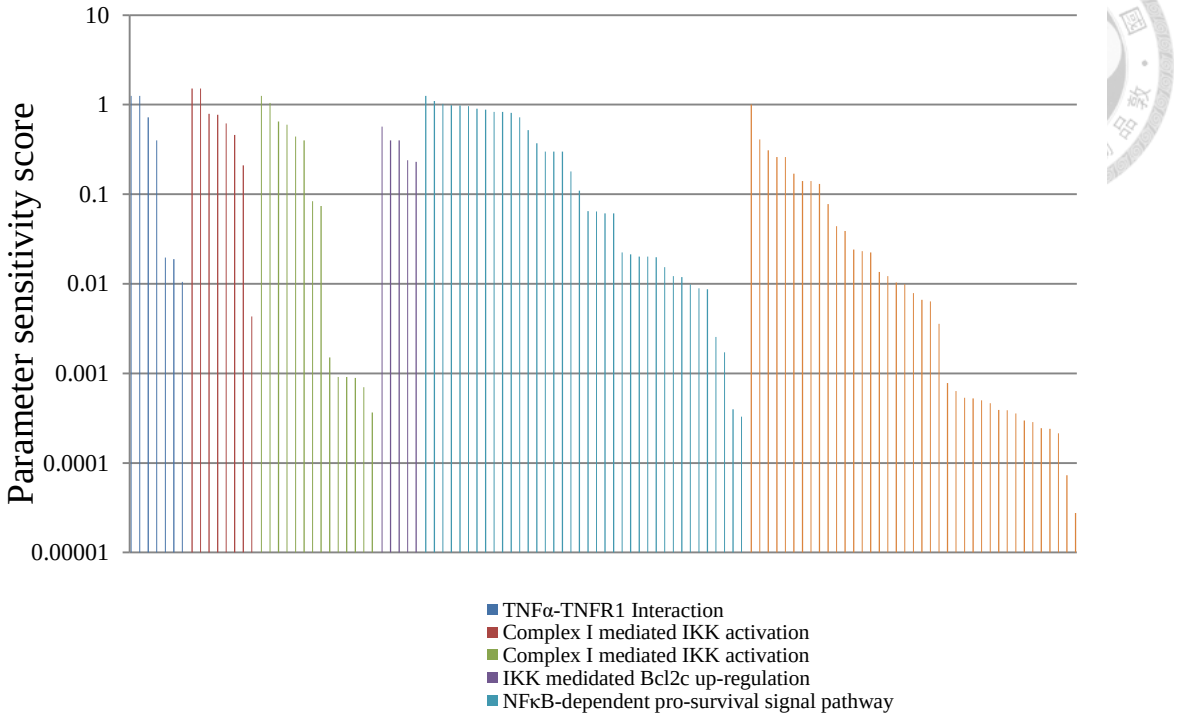

Fig. 15 Sensitivity analysis for parameters in the current model, performed in HeLa cell line setting under TNFα 5 ng/ml treatment.

doi:10.6342/NTU201602117

Table. 1 ANOVA test of parametric sensitivity among 6 groups of parameters, calculated for HeLa cell lines treated with TNFα 100 ng/ml

Subgroup under TNFα 100 ng/ml	Numbers	Mean	Variance	P-value
TNFα-TNFR1 Interaction	7	0.18	0.07	0.09
Complex I mediated IKK activation	8	0.01	4.02×10^{-5}	
Complex II nediated Caspase 8 activation	14	0.16	0.04	
IKK medidated Bcl-2c up-regulation	5	0.03	0.002	
NF-κB-dependent Pro-survival Signal Transduction	38	0.09	0.048	
Extrinsic Apoptosis Pathway	39	0.02	0.025	

doi:10.6342/NTU201602117

Table. 2 ANOVA test of parametric sensitivity among 6 groups of parameters, calculated for HeLa cell lines treated with TNFa 0.5 ng/ml.

Subgroup under TNFα 5 ng/ml	**Numbers**	**Mean**	**Variance**	**P-value**
TNFα-TNFR1 Interaction	7	0.52	0.31	8.8×10^{-5}
Complex I mediated IKK activation	8	0.73	0.30	
Complex II mediated Caspase 8 activation	14	0.32	0.17	
IKK mediated Bcl-2c up-regulation	5	0.36	0.01	
NF-κB-dependent Pro-survival Signal Transduction	38	0.36	0.17	
Extrinsic Apoptosis Pathway	39	0.08	0.03	

doi:10.6342/NTU201602117

Table. 3 Therapeutic Index under the inhibition of IKK mediated Bcl-2c up-regulation pro-survival pathway

Apoptosis rate (%)	**HeLa (%)**	**MEF (%)**	**Therapeutic Index between HeLa and MEF cells**
TNFα=0.01	0	11	0.009
TNFα=0.05	0	31	0.0032
TNFα =0.1	1	13	0.084
TNFα=0.5	18	8	2.23
TNFα=1	25	5	4.92
TNFα=5	15	0	151
TNFα=10	4	0	41
TNFα=100	0	0	1
TNFα=1000	0	0	1

doi:10.6342/NTU201602117

Table. 4 Therapeutic Index under the inhibition of translocation rate of NF-κB from cytoplasm to nucleus

Apoptosis rate (%)	HeLa (%)	MEF (%)	Therapeutic Index between HeLa and MEF cells
TNFα=0.01	0	1	0.091
TNFα=0.05	0	12	0.0083
TNFα=0.1	0	27	0.0037
TNFα=0.5	1	76	0.014
TNFα=1	7	93	0.076
TNFα=5	40	99	0.40
TNFα=10	65	100	0.65
TNFα=100	100	100	1
TNFα=1000	100	100	1

doi:10.6342/NTU201602117

Table. 5 Parameters and reference

Parameter	Value	Reference
csec	1×10-5	Tay et al.
cb	10000	Tay et al.
kb	1.2×10-5	Tay et al.
kf	0.0012	Tay et al.
ka20	1×105	Tay et al.
ka	1×10-5	Tay et al.
ki	0.01	Tay et al.
k1	4.00×10-10	Tay et al.
k3	0.002	Tay et al.
k2	10000	Tay et al.
k4	0.001	Tay et al.
c1	0.1	Tay et al.
c4	0.5	Tay et al.
c4	0.5	Tay et al.
c5	5×10-4	Tay et al.
c3	7.5×10-4	Tay et al.
a2	1×10-7	Tay et al.

doi:10.6342/NTU201602117

a1	5×10-7	Tay et al.
c5a	1×10-4	Tay et al.
i1a	0.002	Tay et al.
e1a	0.005	Tay et al.
kv	5	Tay et al.
tp	0.01	Tay et al.
c6a	2×10-5	Tay et al.
i1	0.01	Tay et al.
a3	5×10-7	Tay et al.
e2a	0.05	Tay et al.
lambda	0.025	Pękalski et al.
c3t	7.5×10-4	Pękalski et al.
c4t	0.05	Pękalski et al.
c5t	2×10-3	Pękalski et al.
csec	1×10-5	Pękalski et al.
cdeg	2×10-4	Pękalski et al.
q1	4×10-7	Tay et al.
q2	1×10-6	Tay et al.
k(12)	1×10-7	Allbeck et al.

doi:10.6342/NTU201602117

kc(12)	1	Allbeck et al.
kbcla	0.0045	Model Fitting
KBcl2c	30	Model Fitting
k(13)	1×10-2	Allbeck et al.
k_(13)	1×10-2	Allbeck et al.
v	7×10-2	Allbeck et al.
k(14)	1×10-6	Allbeck et al.
k_(14)	1×10-3	Allbeck et al.
k(15)	1×10-6	Allbeck et al.
k_(15)	5×10-4	Allbeck et al.
k(16)	1×10-6	Allbeck et al.
k_(16)	1×10-3	Allbeck et al.
k(18)	1×10-6	Allbeck et al.
k_(18)	1×10-3	Allbeck et al.
k(17)	1×10-6	Allbeck et al.
k_(17)	1×10-3	Allbeck et al.
kc(23)	1	Allbeck et al.
k(24)	5×10-8	Allbeck et al.
k_(24)	1×10-3	Allbeck et al.

doi:10.6342/NTU201602117

k(15)	1×10-6	Allbeck et al.
q1t	4×10-8	Pękalski et al.
q2tt	0.002	Pękalski et al.
q2t	1×10-6	Pękalski et al.
q1iap	1×10-6	Model Fitting
q2iap	9×10-5	Model Fitting
c1iap	1	Model Fitting
c3iap	7.5×10-4	Model Fitting
c4rac	2.5	Model Fitting
k(2)	1×10-6	Allbeck et al.
k_(2)	0.001	Allbeck et al.
k(3)	1.8×10-6	Allbeck et al.
k_(3)	1×10-3	Allbeck et al.
kc(3)	10	Allbeck et al.
c5rac	5×10-5	Model Fitting
c4ifip	0.3	Model Fitting
Kflip	800	Model Fitting
k(4)	1×10-6	Allbeck et al.
k_(4)	1×10-3	Allbeck et al.

doi:10.6342/NTU201602117

k(5)	1×10-7	Allbeck et al.
k_(5)	1×10-3	Allbeck et al.
kc(5)	1	Allbeck et al.
k(10)	1×10-7	Allbeck et al.
k_(10)	1×10-3	Allbeck et al.
kc(10)	1	Allbeck et al.
kcDEG37(3)	4×10-4	Model Fitting
k(25)	5×10-9	Allbeck et al.
k_(25)	1×10-3	Allbeck et al.
k(8)	2×10-6	Allbeck et al.
k_(8)	0.001	Allbeck et al.
k(9)	1×10-6	Allbeck et al.
k_(9)	1×10-2	Allbeck et al.
kc(9)	1	Allbeck et al.
kc(25)	1	Allbeck et al.
c4i	63	Model Fitting
Kxiap	80	Model Fitting
kc(8)	0.1	Allbeck et al.
k(27)	2×10-6	Allbeck et al.

doi:10.6342/NTU201602117

k_(27)	1×10-3	Allbeck et al.
k(28)	7×10-6	Allbeck et al.
k_(28)	1×10-3	Allbeck et al.
k(11)	5×10-5	Allbeck et al.
k_(11)	1×10-3	Allbeck et al.
k(19)	1×10-6	Allbeck et al.
kc(19)	1	Allbeck et al.
k(20)	2×10-6	Allbeck et al.
k_(20)	1×10-3	Allbeck et al.
kc(20)	1	Allbeck et al.
k(21)	2×10-6	Allbeck et al.
k_(21)	2×10-3	Allbeck et al.
kc(21)	1	Allbeck et al.
k(22)	1×10-2	Allbeck et al.
k_(22)	1×10-2	Allbeck et al.
k(26)	1×10-2	Allbeck et al.
k_(26)	1×10-2	Allbeck et al.
k(23)	5×10-7	Allbeck et al.
k_(23)	1×10-3	Allbeck et al.

doi:10.6342/NTU201602117

Table. 6 Abbreviationtion of ODE Components

Abbreviation	
TNFRa	active TNFR1 receptors
IKKKa	active form of IKKK
IKKa	active form of IKK
IKKn	neutral form of IKK
IKKi	inactive form of IKK
A20_mRNA	A20 mRNA
A20	cytoplasmic A20
IκBα_mRNA	IkBa mRNA
IκBα	free cytoplasmic IkBa protein
IκBαn	free nuclear IkBa protein
IκBα p	phospo-IkBa cytoplasmic
NFκB	free cytoplasmic NFkB
NFκBn	free nuclear NF-kB
(NFκB :IκBα)	cytoplasmic (NF-kB:IkBa) complexes
(NFκB :IκBαp)	cytoplasmic (phospho-IkBa:NF-kB) complexes
TNF_mRNA	TNFa mRNA
TNF	intracellular TNFa
TNF_ext	extracellular TNFa

doi:10.6342/NTU201602117

G_A20	A20 gene state
G_IkBa	IkBa gene state
G_TNFa	TNFa gene state
TNFRi	inactive TNFR1 receptors
IKKKn	neutral form of IKKK
IKK ii	inactive intermediate form of IKK
(NFκB n :IκBαn)	nuclear (NF-kB:IkBa) complexes
G_Xiap	XIAP gene state
XIAP_mRNA	XIAP mRNA
R*	active receptor complex
flip	FLICE (FADD-like IL-1β-converting enzyme)-inhibitory protein
flip:R*	complex formed by active receptor and flip protein
pC8	Procaspase-8 and Procaspase-10
R*:pC8	complex formed by active receptor and pC8
C8	cleaved procaspase-8 and Procaspase-10; active form of Caspase-8 and Caspase-10
Bar	Bifunctional apoptosis regulator, bind to C 8

doi:10.6342/NTU201602117

	act as an inhibitor
Bar:C8	complex formed by Bar and C8
pC3	Procaspase-3 and Procaspase-7
C8:pC3	complex formed by pC3 and C8
C3	cleaved procaspase-3 and Procaspase-7; active form of Caspase-3 and Caspase-7
XIAP	X-linked inhibitor of apoptosis protein (XIAP)
XIAP:C3	complex formed by C3 and XIPA
PARP	DNA damage repair enzyme; surrogate of all substrates of C3
C3:PARP	complex formed by C3 and PARP
CPARP	cleaved PARP; measure of single cell death
Bid	substract of cleaved caspase-8; inactive form
C8:Bid	complex formed by C8 and Bid
tBid	cleaved Bid; active form
Bcl2c	represents the family of anti-apoptotic Bcl-2 proteins (Bcl-xl and Bcl-2) in the cellure compartment
Bcl2c:tBid	complex formed by Bcl2c and tBid

doi:10.6342/NTU201602117

Bax	substract of tBid; inactive form
tBid:Bax	complex formed by Bax and tBid
Bax*	active form of Bax
Baxm	Bax* at the mitochondrial compartment
Bcl2	represents the family of anti-apoptotic Bcl-2 proteins (Bcl-xl and Bcl-2) in the mitochondrial compartment
Baxm:Bcl2	complex formed by Baxm and Bcl2 in the mitochondrial compartment
Bax2	complex formed by Baxm and Baxm in the mitochondrial compartment
Bax2:Bcl2	complex formed by Bax2 and Bcl2 in the mitochondrial compartment
Bax4	complex formed by Bax2 and Bax2 in the mitochondrial compartment
Bax4:Bcl2	complex formed by Bax4 and Bcl2 in the mitochondrial compartment
M	the number of unoccupied Bax4 binding sites on outrer manbrance of the mitochondria

doi:10.6342/NTU201602117

Bax4:M	complex formed by Bax4 and M
M*	the number of pores Bax4 created on the outrer manbrance of the mitochondria
CytoCm	cytochrome c inside the DIABLO
M*:CytoCm	the numbers of CytoCm at M*
CytoCr	cytochrome c released from the mitochondria, but still in the mitochondria compartment
Smacm	Smac/DIABLO inside the mitochondria compartment
M*:Smacm	complex formed by M* and Smacm
Smacr	Smac/DIABLO released from the mitochondria, but remaining in the mitochondria compartment
CytoC	cytochrome c in the cell compartment
Apaf	apoptotic protease activating factor-1; substract of CytoC, inactive form
Apaf:CytoC	complex formed by Apaf and CytoC
Apaf*	active form of Apaf; complex of
pC9	inactive form pro-Caspase9

doi:10.6342/NTU201602117

Apop	apoptosome ; complex form by Apaf* and pC9
Apop:pC3	complex formed by Apop and pC3
Smac	Smac/DIABLO inside the Cellular compartment
Apop:XIAP	complex formed by Apop and Xiap
Smac:XIAP	complex formed by Smac and Xiap
C3_Ub	C3 ubiquitinated and targeted for degradation

doi:10.6342/NTU201602117